6-2019

Determination of Cleaning Frequency and Power Enhancement of Photovoltaic Panels Using Novel Cleaning Approach

Ali Hasan Shah

UAEU

جامعة الإمارات العربية المتحدة
United Arab Emirates University

United Arab Emirates University

College of Engineering

Department of Electrical Engineering

DETERMINATION OF CLEANING FREQUENCY AND POWER ENHANCEMENT OF PHOTOVOLTAIC PANELS USING NOVEL CLEANING APPROACH

Ali Hasan Shah

This thesis is submitted in partial fulfilment of the requirements for the degree of Master of Science in Electrical Engineering

Under the Supervision of Dr. Mohammad Shakeel Laghari

June 2019

Declaration of Original Work

I, Ali Hasan Shah, the undersigned, a graduate student at the United Arab Emirates University (UAEU), and the author of this thesis entitled "*Determination of Cleaning Frequency and Power Enhancement of Photovoltaic Panels Using Novel Cleaning Approach*", hereby, solemnly declare that this thesis is my own original research work that has been done and prepared by me under the supervision of Dr Mohammad Shakeel Laghari, in the College of Engineering at UAEU. This work has not previously been presented or published or formed the basis for the award of any academic degree, diploma or a similar title at this or any other university. Any materials borrowed from other sources (whether published or unpublished) and relied upon or included in my thesis have been properly cited and acknowledged in accordance with appropriate academic conventions. I further declare that there is no potential conflict of interest with respect to the research, data collection, authorship, presentation and/or publication of this thesis.

Student's Signature: _____ Date: 18/07/2019

Approval of the Master Thesis

This Master Thesis is approved by the following Examining Committee Members:

1) Advisor (Committee Chair): Dr. Mohammad Shakeel Laghari

   Title: Associate Professor

   Department of Electrical Engineering

   College of Engineering

   Signature _____ Date 20-06-201

2) Member: Dr. Addy Wahyudie

   Title: Associate Professor

   Department of Electrical Engineering

   College of Engineering

   Signature addy wahyudie Date 20-06-2019

3) Member (External Examiner): Prof. Tapas K. Mallick

   Title: Professor

   Department of Renewable Energy

   Institution: University of Exeter, UK

   Signature _____ Date 20/6/2019

This Master Thesis is accepted by:

Dean of the College of Engineering: Prof. Sabah Alkass

Signature Mohamed Al Marzouqi Date 18/07/2019

Acting Dean of the College of Graduate Studies: Prof. Ali Al-Marzouqi

Signature Ali Hassan Date 18/8/2019

Copy 2 of 8

Advisory Committee

1) Advisor: Dr. Mohammad Shakeel Laghari

Title: Associate Professor

Department of Electrical Engineering

College of Engineering, United Arab Emirates University

2) Co-advisor: Dr. Ahmed Hassan

Title: Associate Professor

Department of Architectural Engineering

College of Engineering, United Arab Emirates University

Approval of the Master Thesis

This Master Thesis is approved by the following Examining Committee Members:

1) Advisor (Committee Chair): Dr. Mohammad Shakeel Laghari

   Title: Associate Professor

   Department of Electrical Engineering

   College of Engineering

   Signature _____ Date _____

2) Member: Dr. Addy Wahyudie

   Title: Associate Professor

   Department of Electrical Engineering

   College of Engineering

   Signature _____ Date _____

3) Member (External Examiner): Prof. Tapas K. Mallick

   Title: Professor

   Department of Renewable Energy

   Institution: University of Exeter, UK

   Signature _____ Date _____

Abstract

Dust accumulation on photovoltaic (PV) surface decreases the solar radiation penetration to the PV cells and eventually the power production from the PV system. In order to prevent the dust-based power losses, the PV systems are required to be cleaned frequently depending upon different geographical locations, PV integration scheme and the scale of the PV power plant. In large-scale power plants, the PVs are periodically cleaned traditionally by water sprinkling that requires sophisticated equipment mobile equipment that at the best involves robotics and hence calls for substantial capital investment as well as water consumption. Since most of the large-scale PV plants are located away from the urban centres, water transportation required for PV cleaning incurs tremendous overheads thus increasing the electricity production cost. The desert environment that houses utility-scale PV plants in UAE poses a three folds challenge to keep the plant cleaned namely

1. The increased dust accumulation on the PV surface due to sandstorms that requires more frequent cleaning.
2. The lack of water supply infrastructure in the non-populated spaces.
3. The water scarcity that eventually renders water being the most precious resources.

The current project attempts to overcome the grave problem facing PV plant in the desert by proposing an onsite water production employing a PV customized atmospheric water generation (AWG) system. The research involved at first determining the optimal frequency of cleaning within the UAE indicating a minimum of 13 % power loss in UAE within non-sandstorm conditions. The radiation loss due to dust accumulation was calculated by a measured difference in the incident and transmitted radiation through a transparent glass surface. The radiation loss reached up to 27 % within three months during non-sandstorm winter clean sky conditions that represent yet the best-case scenario. The findings enabled designing the optimal capacity of the AWG system.

At a second phase, the AWG designed incorporating diurnal dew point drop, adiabatic air expansion in porous media, radioactive cooling over a sky exposed surface and Peltier cooling in sequential order to achieve an autonomous AWG system. The proposed AWG was constructed and tested with an average water production of 110 ml per night (2-3 hours) having average night-time humidity of 66 % with average electricity consumption of 1.17 kWh/day. The water produced over seven-night reached an average value of almost 1 litre that was sprinkled over the panel and wiped of that achieved completely cleaned PV surface.

Keywords: Radiation, Efficiency, Water Sprinkling, Transportation, Environment, Infrastructure, Radiative, Expansion, Atmospheric, Peltier, Cleaning.

Title and Abstract (in Arabic)

تحديد عدد مرات التنظيف اللازمة لألواح الطاقة الضوئية وتعزيز الطاقة الناتجة عنها باستخدام طريقة تنظيف مبتكرة

الملخص

يعمل تراكم الغبار على أسطح الخلايا الضوئية على تقليل تغلغل الإشعاع الشمسي إلى الخلية الكهروضوئية؛ والذي بدوره يقلل من كفاءة هذه الأنظمة، ويقلل من طاقتها المنتجة. ومحاولة لتقليل كمية الطاقة المفقودة نتيجة للغبار المترسب على أسطح هذه الخلايا الضوئية، يجب ضمان نظافة هذه الأنظمة عن طريق التنظيف المتكرر والدوري؛ وفقًا لمواقعها الجغرافية، ونظام الطاقة الكهروضوئية المستخدم، ومساحة محطة توليد الطاقة الكهروضوئية. ذلك ويتم تنظيف الأجهزة الكهروضوئية في محطات الطاقة الكبيرة بشكل دوري بطرق تقليدية، عن طريق رش المياه باستخدام معدات خارجية متنقلة، تشمل الروبوتات. وبالتالي تتطلب عمليات التنظيف هذه استثمارات رأسمالية كبيرة، وكذلك استهلاكًا كبيرًا للمياه. كما أن معظم محطات الطاقة الكهروضوئية الواسعة النطاق تقع بعيدًا عن المراكز الحضرية، مما يتطلب نقلًا مائيًا لكمية كبيرة من الماء لتنظيف الخلايا الكهروضوئية. تستلزم عمليات النقل المائي، وكمية المياة المستخدمة اللازمين للتنظيف الكهروضوئي لهذه المحطات نفقات هائلة تزيد من تكلفة إنتاج الكهرباء. كما أنّه يتم تثبيت معظم محطات توليد الطاقة الكهروضوئية على نطاق صحراوي واسع، وتشكل البيئة الصحراوية التي تضم هذه الخلايا الكهروضوئية على نطاق المرافق في الإمارات العربية المتحدة تحديًا يتمثل في التالي:

1- زيادة تراكم الغبار على أسطح الخلايا الضوئية؛ بسبب العواصف الرملية والذي بدوره يتطلب تنظيف أكثر تواترًا.

2- نقص البنية التحتية لإمدادات المياه في الأماكن غير المأهولة بالسكان.

3- ندرة المياه التي تجعل المياه في نهاية المطاف هي أثمن الموارد.

يهدف هذا البحث لإيجاد طريقة للتغلب على هذا القيد من خلال آلية بديلة لإنتاج المياه في موقع تثبيت الخلايا الضوئية بتطبيق نظام مخصص لتوليد المياه من الغلاف الجوي. وبتحديد التكرار الأمثل للتنظيف في دولة الإمارات العربية المتحدة، أشارت النتائج إلى فقدان الطاقة بنسبة

13٪ كحد أدنى في ظل ظروف غير عاصفة رملية. كما بلغت نسبة فقدان الإشعاع الناتجة عن تراكم الغبار عن طريق حساب الفرق بين الإشعاع المنتج والإشعاع المنقول عبر سطح زجاجي شفاف. بلغ فقدان الإشعاع ما يصل إلى 27٪ في غضون ثلاثة أشهر خلال ظروف السماء النظيفة الشتوية غير العاصفة، التي تمثل حتى الآن السيناريو الأفضل. وحيث أن النتائج السابقة مكنت تصميم السعة المثلى لنظام AWG.

و في المرحلة الثانية، فإن تجسيد نظام توليد المياه في الغلاف الجوي سوف يستغل انخفاض نقطة الندى النهارية ، وتمدد الهواء الساكن في الوسط المسامي، والتبريد الإشعاعي على الأسطح المكشوف باتجاه السماء، وبلتيير برودة بترتيب متسلسل لتحسين نظام التنظيف الكهروضوئي الذي يعتمد على نفسه. تم إنشاء واختبار AWG المقترح بمتوسط إنتاج للمياه يبلغ 110 مل في الليلة (2-3 ساعات) مع متوسط رطوبة في الليل بنسبة 66٪ مع متوسط استهلاك للكهرباء يبلغ 1.17 كيلو واط في الساعة. بلغت قيمة المياه المنتجة على مدار سبع ليال متوسط 1 لتر تقريبًا تم رشها على اللوحة ومسحها مما أدى إلى تنظيف سطح الخلية الضوية بالكامل.

مفاهيم البحث الرئيسية: الإشعاع ، الكفاءة ، رش المياه ، النقل ، البيئة ، البنية التحتية ، الإشعاعية ، التوسع ، الغلاف الجوي ، التنظيف.

Acknowledgements

First, I would like to express my graduate to “Allah Almighty” for bestowing countless blessings, opportunity, determination and strength to achieve this milestone.

This thesis would not have been possible without the guidance and help of my advisors Dr. Mohammad Shakeel Laghari and Dr. Ahmed Hassan, I pay my deep regards and gratitude for their continuous support, help and knowledgeable pieces of advice throughout this study. I would like to thank my Academic Coordinator Dr. Mousa Hussein and Graduate Office who supported to format the thesis according to the predefined standards and helped me to present my work in a better way. I am also grateful to Dr. Addy and Dr. Tapas K. Mallick who gave their suggestions to improve thesis report.

I am very thankful to the Electrical Engineering Department faculty for feeding knowledge and nourishing my skills. I would also like to thank United Arab Emirates University for giving me the platform to pursue my studies and research work.

I would like to thank my dear wife Seerat Fatima, and colleagues and friends Qamar Navid, Shaimaa Abdel Baqi, Muhammad Omar, Yasir Rashid, Muhammad Usman, Muhammad Zeeshan and Muhammad Rehan for discussions, suggestions and encouragement. Saad Saleem deserves my special thanks as he helped me developing the algorithm and motivated me throughout this period.

I would be nothing without the love and support of my family and my final words go to my brothers Saeed Ahmad Shah and Naveed Hassan Shah who were behind my all success stories.

Dedication

To my loving mother and father (late)

Table of Contents

List of Tables

List of Figures

List of Abbreviation

AC	Alternating current
Amb	Ambient
AWGS	Atmospheric water generation system
C	Cleaning
C_d	Module cleaning on a daily basis
C_{10_d}	Module dusted for 10 days
C_{20_d}	Module dusted for 20 days
C_m	Module dusted for a month
C_{3_m}	Module dusted for 3 months
DAQ	Data acquisition
DC	Direct current
Eq	Equation
FF	Fill factor
NI	National instruments
PV	Photovoltaic
TEP	Thermoelectric Peltier

Symbols

A	Area (m^2)
d_c	Dusting coefficient
h_c	Heat coefficient
I_{sc}	Short-circuit current (ampere)
T	Temperature (°C)
V_{oc}	Open-circuit voltage (V)
G	Global solar radiation intensity (W/m^2)
H	Latent heat of fusion (kJ/kg)
P	Power (W)
Q	Energy (Kwh)
V	Volume (L)
V_w	Wind speed (m/s)
α	Absorptance of clear glass (%)
ρ	Density (kg/m^3)

Chapter 1: Introduction

This introductory chapter gives the objectives of the current research, the methodology used to conduct the research and its futuristic impact. It also includes the structure of the thesis report.

1.1 Objectives of the research

The main objectives of this research are to design a water-based PV cleaning mechanism that generates onsite water through a customized atmospheric water generation system. In order to produce an optimal design, the determination of the actual dust-based radiation and power losses over time are important goals of the research. The finding is intended to determine the cleaning PV frequency that eventually will help determine the amount of water required for the PV cleaning over a period of time through experimentation (Specifically in UAE conditions). The required amount of water would help to design the capacity of the "atmospheric water-generation system" for cleaning of the solar panels and its fabrication according to the design.

To achieve these objectives, an array of PV panels was installed at the site and the dust-based radiation and power losses were measured on a daily, weekly, monthly and seasonal basis. The atmospheric water-generation system and self-cleaning mechanism for solar arrays were developed to prevent dust driven power losses and solar cell deterioration from the dust build up over the panels.

This research has been guided by a sensitivity analysis of the frequency of cleaning compared to the loss of power that would occur due to non-cleaned panels. A fine balance was identified between the cost of increased frequency of cleaning

involving human resource, equipment and energy overheads compared to the cost of power losses due to delayed cleaning through experimentally measured data. The research adds a substantial contextual value in relation to UAE climatic conditions which warrants more frequent cleaning due to prevalent desert environment and episodes of dust storms.

1.2 Methodology

An array of PV panels was installed at the site to measure the cleaning frequency. The effects of dust accumulation on PV panels in terms of loss of radiation incident on PV cells and power loss caused by the reduced incident radiation was measured over a pre-defined period of time. National Instruments Compact DAQ and modules are used to measure the currents, voltages and temperatures of PV panels for the dusty and cleaned panels after a pre-defined frequency. Temperature distribution over the surface of PV panels was studied through thermography by using the infrared camera. The vintage pro weather station was used to measure the weather data comprising of wind speed, ambient temperature and air humidity.

These weather data findings were utilized to design an optimal capacity of the atmospheric water generation system. The embodiment of atmospheric water generation system exploited the diurnal dew point drop radiative cooling over a sky exposed surface and Peltier cooling in sequential order to optimize the self-reliant PV cleaning system. The atmospheric water generation system integrated with the PV panels to clean the dusty panels after a calculated timespan.

1.3 Research impact

This work mainly focuses on the efficiency enhancement of PV panels by cleaning the PV panels after the measured time period by integrating the atmospheric water generation system into the PV system.

This project is aiming for the betterment of society at the global scale and the outcomes are in the following manners:

- The research informed about the time duration that warrants cleaning the PV panels that eventually reduced the cost related to PV cleaning.
- A prototype test set up was fabricated to produce water, embodying the concept of dew point, condensation over a radiatively cooled surface and electrically powered Peltier cooling effect.
- The research designed a process of PV cleaning intended to reduce the overhead associated with water utility required for PV cleaning equipment.
- The research helped to recover the power losses caused by PV soiling.
- The research also aided to improve the overall efficiency of the system.

1.4 Thesis structure

This study is divided into six chapters. Chapter 1 (Introduction) gives the objectives of the current research, the methodology used to conduct the research and its futuristic impact.

Chapter 2 presents an extensive review of the current and future energy needs and its generation and consumption. Mainly, discussing the use of solar photovoltaic technology and its benefits, different factors (solar spectrum, reflection, temperature and soiling) that affect efficiency are described in detail. It concludes the literature review on soiling losses and different cleaning techniques.

Chapter 3 presents the details of different materials, devices and facilities used to conduct the research.

Chapter 4 describes the experimental setup, execution of the experiment and detailed analysis of the results to measure the cleaning frequency of PV panels.

Chapter 5 provides the design of atmospheric water generation system and how to exploit the diurnal dew point drop, radiative cooling over a sky exposed surface and Peltier cooling in sequential order to optimize the self-reliant PV cleaning system. It also described the Simulink modelling of the AWG system with a detailed analysis of the results.

Chapter 6 represents the conclusions of the results drawn from the experiments and recommendations for future research based on these results.

Chapter 2: Literature review

This chapter presents an extensive review of the current and future energy needs and its generation and consumption. Mainly, discussing the use of solar photovoltaic technology and its benefits, different factors (solar spectrum, reflection, temperature and soiling) that affect efficiency are described in detail. It concludes the literature review on soiling losses and different cleaning techniques.

2.1 World energy needs and solar power

Due to the rapid economic development, industrialization and surge in population, the consumption and demand for energy increasing at a substantial rate [1]. According to the ‘‘Global Energy Statistical Yearbook 2018’’ the world total energy and electricity consumption was 8561 Mtoe (million tons of oil equivalent) and 9984 TWh respectively in 1990, which reached up to 13730 Mtoe and 22015 TWh in 2017 with the increase of 38% and 55% respectively. The world total electricity consumption according to the regions from 1990 to 2017 is shown in Figure 1 [2].

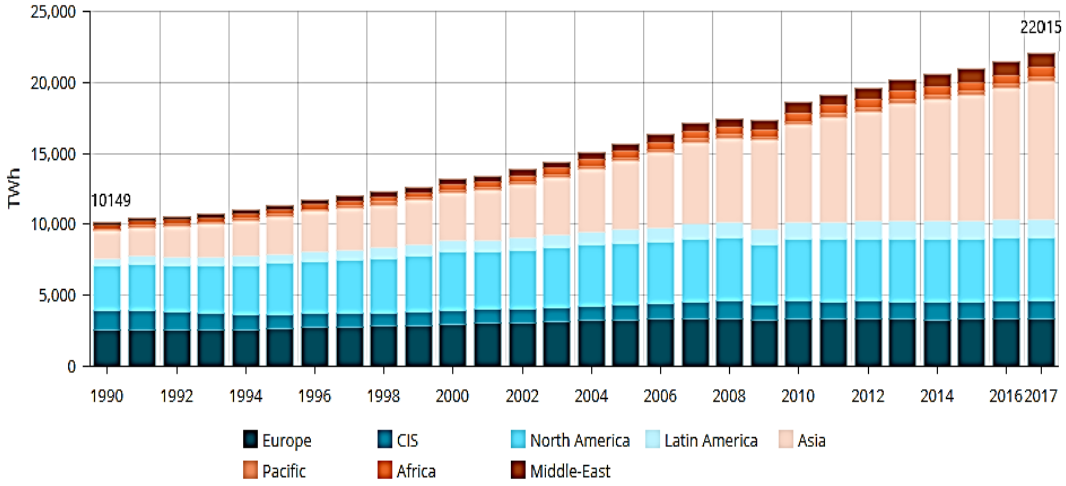

Figure 1: World total energy consumption from 1990 to 2017.

Fossil fuels (oil, coal and gas) are the major contributor to fulfil the world energy needs [3]. The burning of fossil fuels causes the emission of carbon dioxide CO_2, as it was 32668 $MtCO_2$ in 2017. Carbon emission has very serious implications for the climate and human health, such as glacial melt, more extreme weather, ocean current changes, acid rain, acidification of the ocean and consequent damage to the ecosystems and health of living organisms [4]. Recently, the world is increasingly departing from fossil fuels to renewable energy sources to prevent the release of carbon dioxide and to achieve the needs. The renewable energy sector is growing faster with currently providing 25% of total energy demand and expected to rise up to 30% in 2023 according to the ‘‘International Energy Agency’’ (IEA) as shown in Figure 2 [5].

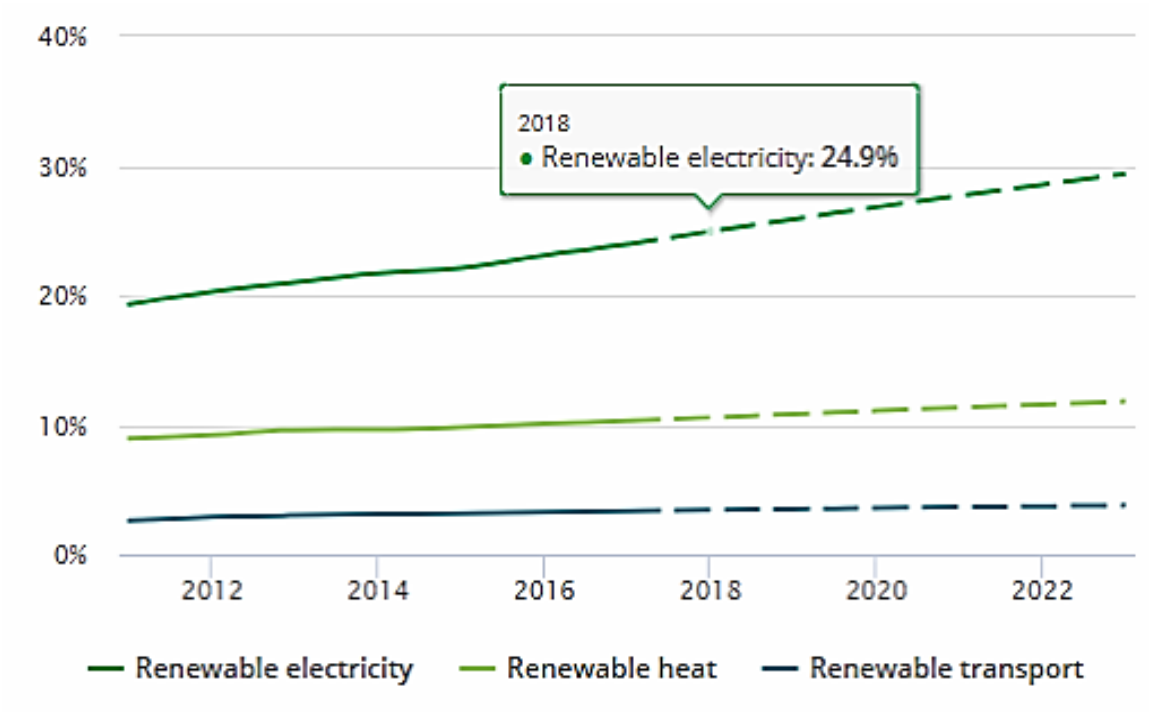

Figure 2: Share of the renewable energy sector in the global energy mix by sector from 2011-2023.

Photovoltaic is one of the most rapidly growing technology compared to all other renewable technologies supported by a rapid cost decline and efficiency improvement in addition to reducing greenhouse gasses emission and saving the environment [6]. Since 2010, the prices for large utility-scale PV plants have fallen by 70% thus increasing power generation to 460 TWh bringing it up 2 % share in the world energy generation which is expected to increase rapidly in coming years. Record growth of 98 GW in solar photovoltaics in 2017 was driven by China's quick deployment with 53 GW of capacity, backed by feed-in tariffs incentives. Despite the surging annual market, average PV prices are expected to continue to decline in the coming years as competition increases and manufacturing capacity grows in China and South East Asia. More than two third of the world's PV modules are currently being produced by Chinese companies. The USA continues to be the second largest PV market after China. India's annual PV additions more than doubled, with 9.6 GW coming online. In the European Union, annual PV additions remained stable at 6 GW [7].

Because of the above-stated developments, solar PV investment reached its highest level ever in 2017, at over USD 160.8 billion encouraged by a decline in capital costs of new installations by 25% [8]. According to the IEA report, the sun might be the single largest source of energy generation by reaching 16% of world energy supply by 2050. There are many energy sources which are being used to produce electricity but most of them involve serious problems like high pricing, pollution and the deficiency of the resources with the time. While the sun is a clean, green and free source of energy which has edge benefits of other conventional ways to produce electricity in different aspects.

Solar energy is very beneficial for the environment because it does not contaminate it like other conventional energy sources (coal and oil powered power plants) which cause the generation of millions of tons of waste, emission of greenhouse gasses and different harmful substances which has high concerns of health [9, 10] . As the sun is a renewable energy source and its energy not going to decrease with the time like the other conventional power production sources which consuming fossil fuels for power generation. Fossil fuels including oil, gas and coal are the finite sources and currently are the world's primary source of energy and are going to be finished in future. While solar energy is purely a renewable energy source and can easily meet the energy needs of our future generations [11, 12]**.** The impact of solar energy or renewable energy industry on employment is still debatable. But according to the results gathered by conducting the different surveys worldwide shows the as the demand of renewable increasing rapidly, photovoltaic industry generating more jobs than the average job increases worldwide, which varies region to region [13].

It's already a well-established fact that renewable sources of energy are clean and cost-effective than other conventional energy sources. These also offer the potential of energy independence and security because no country will be dependent on the other country for energy resources. For example, some country is producing its own electricity by using renewable energy coming from the sun, means they are not depending on oil, coal and gas coming from other countries. So, by using solar energy, electricity can be generated to fulfil the energy requirements without compromising security [14]. Currently, the cost of solar panels is hundred times low than the cost in 1877. Using the PV panels as an electricity source are cost-effective in different means e.g. PV panels provide protection from continuously rising energy prices and savings in electricity bills. The cost of PV is down to $0.10 per KwH, in contrast, the generated

energy from fossil usually falls to $0.05 to $0.17 per KWH. According to the IRENA's Renewable Power Generation Costs in 2017 report the cost of solar PV will fall further halve of typical cost in the future by 2020. This means that in two years ' time, onshore wind and solar PV projects could consistently supply electricity for just under $0.03 per kWh [15].

2.2 Photovoltaic system

Energy demand is growing rapidly with the passage of time. Current power consumption in the world is 22 terawatts hour (TWh) per year and it is projected to be 40 TWh in 2050 and more than triple at the end of this century according to the data provided by "Enerdata" in "Global Energy Statistical Yearbook 2018" [16] . The fossil fuels that currently we are consuming will not last long to fulfil our requirements of energy consumption in future. Additionally, their continuous use produces numerous side effects and pollutes the environment. We have a sun as an abundant and clean source of energy. The sun transmits 120,000 TW of energy on the earth's surface, being much higher than our consumption.

Photovoltaic cell invented in 1954, when D. Chapin, C. Fuller, and G. Pearson demonstrated solar cells based on P-N junction with efficiency 5-6% [17]. Photovoltaic (PV) cells are the semiconductor devices, which have the ability to convert energy carried by solar radiation into DC electricity [18]. Solar radiations strike at the cell surface and the cell converts these radiations into electricity. The sunlight conversion in electricity is called a photovoltaic effect [19, 20]. Up to 80% of solar radiation can be absorbed by PV cells from the accessible solar spectrum. The larger part of usable radiation belongs to the visible spectrum because the radiations with high and low wavelength do not contribute to electrical energy conversion process

[21]. The DC produced by PV is converted to alternating current (AC) through an inverter [22]. The photovoltaic system thus comprises of solar panels, wirings, charge controller, energy storage battery and inverter as shown in Figure 3. PV panels convert solar energy into DC and that DC power goes to the charge controller.

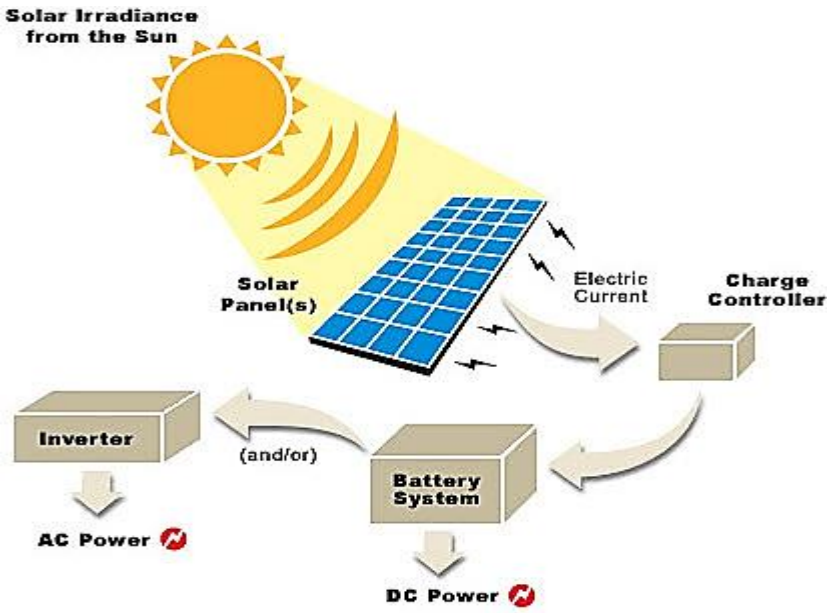

Figure 3: Solar power energy conversion process.

2.2.1 Structure of PV panel

A solar panel is a sophisticated “sandwich”, made up of different layers of materials as shown in Figure 4.

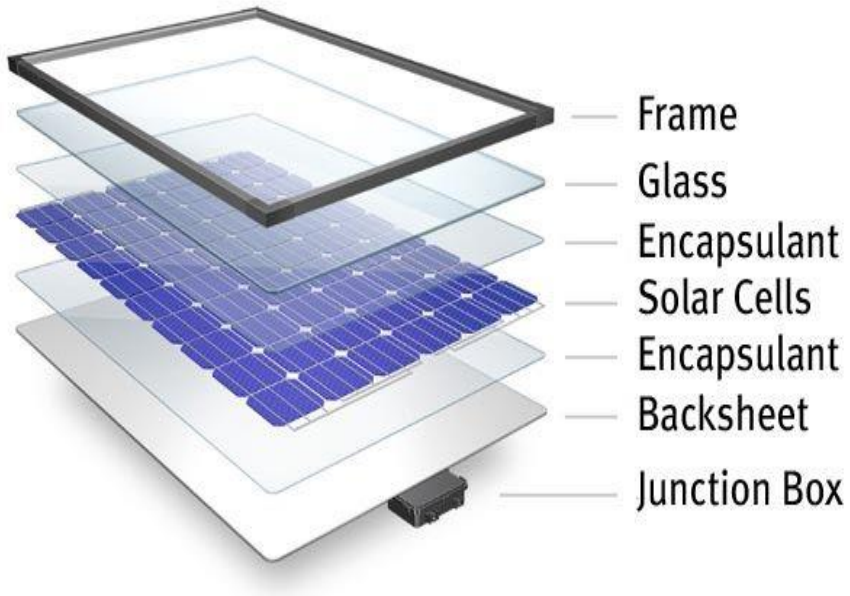

Figure 4: Photovoltaic structure and its layers.

Fundamentally, the frame of the solar cell is used to protect the internal components from thermal and mechanical tension, along with, providing the mounting points. The PV frame structure must be projectionless. Usually, PV frames are made of aluminium, however, replacing metal frames with lightweight high-performance polymers can offer important advantages to solar manufacturers as these are easier to assemble and eliminate outdoor corrosion issues associated with metals as well [24].

A top layer of PV panels is made up of low iron glass which protects the PV panel from different impact, pressure and temperature. The thickness of the front surface glass is between 3.2 mm to 4 mm depending upon the type of chosen glass. It must have the high transmittance of the light in the wavelength range of 350 nm to

1200 nm. To enhance the penetration of sunlight in PV cell the reflection of the front glass must be lowered [25, 26].

Encapsulants material in PV provides long-term protection against environmental stress to the most sensitive portions of solar panels and circuitry. Solar cells are sandwiched between the two layers of the encapsulant. It also provides optical coupling and enables the transmission of sunlight to the solar cells [27].

Crystalline-silicon wafers are the main part of PV panels and they have the ability to capture and convert sunlight into electrical power. Based on their manufacturing process, the silicon crystalline wafers are mainly divided into two categories; monocrystalline solar cells and polycrystalline solar cells. Several emerging cell types such as inorganic cells, amorphous cells, microcrystalline silicon cells, quantum dot cells, organic tandem cells and perovskite cells are also being developed. Monocrystalline cells have higher efficiency than polycrystalline while polycrystalline offer a lower price and thus dominate the market share. The efficiencies of solar cells improved significantly in recent years due to the development of technology and inventions of new materials [28].

Back sheets are used at the back side of PV modules and have direct contact with the environment. These are critical to the long-term durability and protect solar panels from UV, temperature, and moisture effects. These are made of different polymer materials and inorganic modifiers. They also isolate the cells and electrical connections from the environment to enhance performance and safety [29, 30].

The junction box is usually installed at the back of solar modules that protect the electrical wires which carry the current produced from the solar panel to an inverter, where the direct current (DC) is converted to alternating current (AC)

electricity. Wires connected through diodes inside the junction box provide an easy way to link panels with each other [31].

2.2.2 Charge controller

A charge controller in the energy conversion process is a significant component that is used to manage the solar power drawn from the PV panels. If connected to energy storage batteries, it prevents the batteries from overcharging during the day time and make sure that the voltages from the batteries will not flow back to the PV panels when PVs are producing less voltage (usually at the evening time) than the stored voltages of batteries. Many charge controllers change the voltages and current from the PV panels to batteries according to the state of charge of the battery.
Mainly these are separated into two categories [32]:

- Pulse Width Modulation (PWM)
- Maximum Power Point Tracking (MPPT)

MPPT has a performance advantage over the PWM charge controller and is used to draw maximum power from the PV panel to feed either the load or charge the battery depending on the PV system configuration [33].

2.2.3 Solar inverter

As most households require AC supply to perform the function, the DC output from the PV panels requires to convert the DC to AC through solar inverters. The rating of inverter should be 1.5 times higher than the PV panels rated output to acquire the peak power in peak hours.

2.3 Factor affecting PV conversion efficiency

When solar radiations strike at the surface of the PV panel, it converts this photon energy into electrical power. PV panels do not convert all the striking radiation into electrical power as most of the radiations get wasted due to several factors that affect the PV panel performance. Major factors that affect the conversion efficiency of solar panels are dust accumulation, module temperature elevation, sunlight spectrum, panel direction and tilt angle. The detailed discussion on how these factors affect the PV panels' conversion efficiency is provided in the sections below.

2.3.1 Solar spectrum

When the sunlight hits the semiconductor material and penetrates into it, if the band gap energy of a striking photon is equal to or greater than the semiconductor material bandgap energy then it sets electrons free and thus generates the charge carriers in the forms of mobile electrons and holes [34]. The selective solar spectrum portion is absorbed by these semiconductor devices. Only the visible part which has the wavelength range 400 nm to 700 nm generates the electrical current after penetrating in solar cells. The electric current generated by PV modules depends on the spectral sunlight distribution and the effects of the solar spectrum on PV performance depends on metrological conditions, the sun position and module mounting type [35]. The visible region is more than the UV and the infrared region is involved in creating short-circuit current. As the visible region of striking radiations decreases and infrared and UV regions increase, the generated current also get decreases that ultimately effects the power produced by the module [36, 37]**.** PV cells are not highly efficient as they are unable to respond to the whole spectrum of solar radiations. If the photon energy of striking radiations is less than of band gap energy

of the cell material, then it gets absorb but do not contribute to creating the charge carriers. If the photon energy is larger than the material bandgap energy, it will get absorbed but these absorbed photons cannot be used effectively due to electrons thermalization. These spectral losses can reach up to 50% in single junction solar cells [38].

2.3.2 Reflection

In photovoltaic technology reflection and absorption losses are included in the main causes of energy loss [39]. By decreasing the amount of reflected light from the solar module surface, the PV panel efficiency can be enhanced. The angle of incident of sunlight is directly associated with the reflection related losses in solar panels [40, 41]. Early in the morning and late evening, the sunlight has a large angle of the incident with respect to the PV panel which causes the increase in reflection related losses. That's why the PV modules produce low power at these time slots. During the all remaining time of the day the optical losses remains almost the same due to the slight difference in the range of $\Theta_{in} > 45°$ [42].

There are several means to decrease optical losses:

- Anti-reflection coatings (ARCs) used on the top surface of the solar cells help reduce the light reflection related losses. Different types of ARCs are being used in the solar cell industry, such as SiNx, Al_2O_3, ZnS and MgO etc.

- Surface texturing is also being used to reduce reflection losses. When the sunlight strike at the textured surface, it reduces the chances of bouncing back the incident light into the atmosphere by trapping it in the surface. This can be used separately or with the combination of ARCs to diminish the reflection losses. Surface texturing can be accomplished in several ways. Texturing of

the single crystalline substrate may achieve by etching onto the faces. If the surface is aligned with internal atoms appropriately, a crystalline structure of silicone results in a pyramidal surface [43, 44].

- The uses of both the light trapping and surface texturing simultaneously may increase the path of light in the cell that will enhance the chance of penetration.

Most of the usually incident lights reflected by a pyramidal texture appear at an angle of 38.9°. This reflected light will be confined to total internal reflection and will likely be absorbed as a second opportunity by a solar cell under an encapsulate with a refractive index n>1.59. This will increase the short circuit current by about 0.39 mA cm^{-2} [44].

2.3.3 Temperature

Temperature elevation effects the photovoltaic in the following ways:

- It causes to drop in open circuit voltages (V_{OC}), maximum power point and overall PV panel efficiency.
- The photovoltaic panel has faster degradation when installed at a hotter climate compare to the cooler.

In the conversion process, the operating temperature of the photovoltaic panel has an important role. According to NREL report 2019, crystalline silicon solar cells convert ~21.2% to 26.6% of incoming solar radiations into electrical energy [45], from the remaining some is reflected back into space and the rest is converted to thermal energy [40]. As discussed earlier, only the visible part of solar radiations contributes to electrical energy conversion while the infrared and ultraviolet radiations convert to heat and eventually results in temperature elevation of solar panels [46]. As

temperature increases, it diminishes the bandgap energy with resulting increased charge mobility while paradoxically reduced V_{OC}, this ultimately reducing the overall PV power output. Due to temperature elevation, the efficiency drop in silicon solar cell reaches up to -0.08%/K and the power drop remains within 0.4 – 0.5%/K [47]. The performance of solar cell varies as the radiations and the ambient temperature along with other factors. The solar panel with the same power rating performs differently at different geographical locations due to the change in radiations level and ambient temperature [48].

Figure 5 shows the effects of temperature rise in terms of voltage and power drop. It has been shown clearly that at ambient temperature -25°C and solar radiation intensity of 1000 W/m^2 the output voltages of the PV panel are almost 25 V. As the T_{amb} increased up to 75°C the output voltages decreased to 17.5 V respectively which eventually leads to a decrease of power according to ohm law [49].

$$P = VI \qquad \text{(Eq. 1)}$$

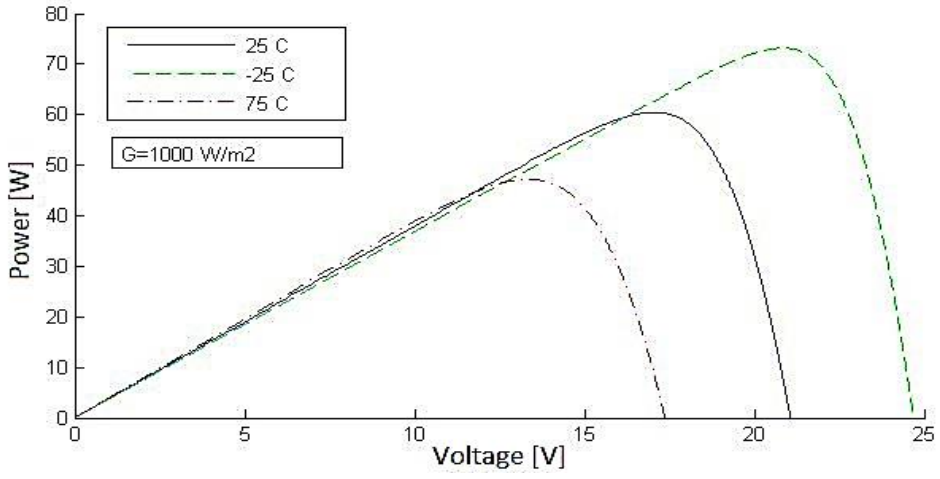

Figure 5: Effects of temperature on the P-V curve.

2.3.4 Dust accumulation

Photovoltaic solar modules produce energy that has a direct relation with the available radiations of the sun [50]. However, regardless of its intrinsic absorption ability, the efficiency of a solar panel will deteriorate over time due to the component performance, accumulation of dust and dirt on its surface [51, 52]. A variety of research studies shows that the soiling substantially diminutions the performance, electrical power and efficiency of the photovoltaic cells [53, 54, 55, 56, 57]. Soiling losses refer to the loss in power resulting from snow, dirt, dust and other particles that cover the surface of the PV module. Dust is a thin layer covering the solar panel surface, and the typical dust particles have a diameter of less than 10 μm, but this mainly depends on the location and environment. The dust comes from a wide range of sources, including wind, pedestrian, motor movement, volcano eruptions etc. The dust accumulation increases the soiling effects over time and affects the total energy generated by the PV module.

There are two primary factors that examine the effect of dust on PV performance, the properties of the dust and the local environment in which the PV system is installed. The dust properties include the size, shape and colour of the particles. The stickiness of the dust particles at any surface also varies from sample to sample. The local environment comprises of the system installation location, means the system is installed in dessert, grassy, plan or mountain region and the height of the installed system from the ground. It also includes the weather conditions like humidity and wind speed, which effects the adhering of dust particles at the surface of modules [58].

The adhesive and rough PV module surface is more probable to build up dust than a less adhesive and smoother surface. It is also a fact that the dust causes to increase the dust if the initial layer of dust deposited at any surface, it provides better ground for the other dust particles to stick there, means the surface is becoming more dust friendly. Horizontal surfaces tend to build up more dust than vertical and tilted ones due to the effects of gravity. This is also depending upon the speed and direction of the wind. Winds with low speed generally support the dust accumulation at the module surfaces, while the winds with high speed remove the dust and clean the surfaces instead. However, the dust accumulation at the PV surface varies according to the geometry of the installed PV system and the direction and speed of the winds at that specific geographical location [59].

Fine and coarse particles have been caught up by horizontal panels, while only fine particles of dust are caught by vertical panels as studied experimentally in [60]. Both quantitative [58] and qualitative [55] methods are applied to understand the deposition of dust particles over the PV surface in various climates and PV tilt. The effects of tilt angle on the deposition of dust particles on PV panel front surface and the relationship between output power, dust particle size and irradiance were studied by [61, 62] experimentally and mathematically. The literature on the frequency of cleaning solar panels from accumulated dust is limited. As, [55, 58] suggests cleaning cycles for PV panels installed in different climate zones based on their weather and dust level.

2.4 Methods of dust removal

The traditional cleaning methods include mechanical cleaning involving air or water flow [63], nano-film based self-cleaning [64] and electrostatic precipitator cleaning [65].

Nano-film based self-cleaning exploits hierarchical nanostructures created on the surface of the glass by combining large honeycomb nano-walls with ultrathin nanorods. The dimensions of these structures are specifically selected to maximize the overall light absorption efficiency. The nanorods serve to reduce the surface reflectance and facilitate light penetration into the cell while the honeycomb structures enhance photon absorption by acting as effective scattering centres. Furthermore, due to its extreme hydrophobicity, the nanostructured packaging glass efficiently repels dust particles, preventing drops in efficiency over time [51].

The electrostatic cleaning involving non-contact mechanism cleans efficiently and protects the top surface of the panel without any physical contact. An electrostatic precipitator removes fine dust particles from the PV panel's surface by using the force of an induced electrostatic charge.

The nano-film and electrostatic precipitator-based methods have limitations to remove dust and cannot effectively clean in humid climates where the dust stucks firmly to the surface. The mechanical methods are more widely used and applicable in a variety of climates due to the reliability of dust removal force, rapid operation and enhanced performance independent of the environment.

Mechanical method is mainly divided into three categories:

- Manual cleaning
- Vacuum suction cleaning
- Automatic wiper based cleaning

Manual cleaning requires the human operator to clean the PV panel manually using water and wiper with the adequate supporting structure. The surface cleaning quality is evaluated by the operator himself on a visual basis to a satisfactory stage or until the particles are totally washed away [66]. A vacuum suction cleaner includes an air pump that creates a partial vacuum for the suction of dust and dirt particles from the surface. The vacuum cleaner motor is generally supplied with electrical power to create suction pressure. Only surfaces outside the corners are correctly cleaned by the vacuum cleaner and it's also operated manually [67]. The automatic cleaning using wipers consist of a water pot to spray the water at PV surface and a rubber wiper to clean that surface. This system operates automatically and needs a power supply to perform functions [68]. However, the mechanical cleaning systems suffer from lack of water supply infrastructure to keep the plant cleaned ending up with massive investments in procuring and operating the cleaning equipment [67, 69].

2.5 Problem identification and proposed solution

A variety of research studies consistently shows that the soiling considerably deteriorates the performance, electrical power and efficiency of the photovoltaic cells. Most of the utility-scale PV power plants are installed in the desert to optimize land use and shading the PV panels from surrounding to maximize solar radiation gains. The desert environments, however, on one hand, dust the panels frequently and lacks water infrastructure for cleaning that eventually ends up cleaning being very expensive.

The ongoing scarcity of water around the world and the recent drought in different regions have led to a surge of new research on water technology. Different methods have been used to produce the water from the atmosphere such as the artisanal method of fog harvesting, air condensation by cooling down the air below the dew point, pressurizing the air or exposing it to the desiccants. Among these methods, most of them required a regular power source to run the water generation system.

Chapter 3: Devices and materials

This chapter includes the details about the materials, devices and facilities used for this research. It also discusses the basic methods to test and characterize the devices and materials used in this study. Below is a list of devices and materials used during the experimentation. It's mainly divided into three categories:

- Energy system
- Measurement system
- Cooling system

3.1 Energy system

Energy system consists of the PV panels and glass modules which are used to measure the cleaning frequency of the system.

Six monocrystalline photovoltaic modules with dimensions of 99 cm x 134 cm, rated capacity of 160 W and module efficiency of up to 17%, were installed outdoors at Al Ain in renewable energy laboratory, UAE University Falaj Hazza Campus, at latitude and Longitude of 24.9° N - 55.5° E respectively. The electrical performance of the modules was confirmed by measuring open circuit voltage (V_{OC}) and short circuit current (I_{SC})prior to inclusion of the PV into the system.

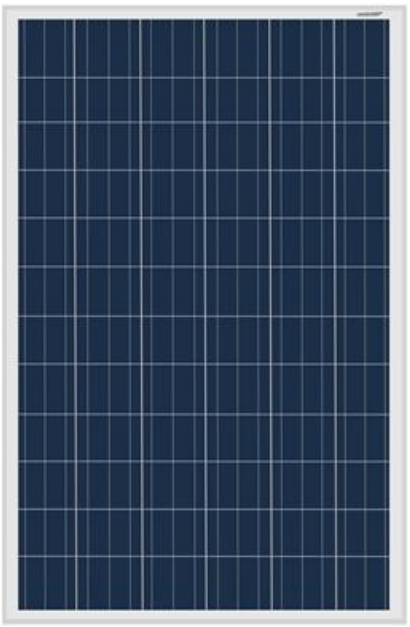

Figure 6: Photovoltaic panel.

PV specifications from the manufacturer are listed below in table 1.

Table 1: Used PV panel specifications.

Solar cells	**Polycrystalline silicon**
Dimension	99 cm x 134 cm
Maximum Power	160 W
Open circuit voltage (V_{OC})	43.32 V
Short circuit current (I_{SC})	5.05 A
Rated voltage (Vmpp)	36.20 V
Rated current (Impp)	4.59 A

3.2 Measurement system

Measurement systems included different measurement and logging devices that are used to measure the different parameters and log the data with the help of software. Below is the list and description of used devices:

- Data acquisition system
- LabVIEW software & Desktop
- Weather station
- Thermocouples
- Pyranometers

3.2.1 Data acquisition system

DAQ is an inform DAQ is an information system consisting of software and hardware, as well as the information collection, storage and distribution with the help of sensors and actuators. It is used to measure voltage, current, temperature, pressure interfaced with LabView. The input is connected to the DAQ hardware, the signal is transmitted from the input device to the hardware that processes and sends it to DAQ software for further analysis and examination. For the measurement of temperature, thermocouples are connected with DAQ and the measuring surface (PV). The temperature is measured in the form of voltages that later is converted to temperature values through a calibrated equation in the DAQ measurement hardware using programmable software.

The NI DAQ Pro_cDAC-9174 is used in these experiments for data acquisition. This chassis can accommodate up to 8 slots (temperature, voltage, current). The modules NI-9213, NI-9227 and NI-9221 are used to measure temperature, current and voltages respectively in this research [70].

Figure 7: The NI DAQ Pro_ cDAC-9174.

The module NI-9213 shown in Figure 8 is a thermocouple input module with ±1.5 (°C) accuracy. It has 16 input channels, along with -75°C – 250°C measurement range, 24-bit ADC for up to 0.02°C measurements sensitivity [71].

Figure 8: The module NI-9213 to measure temperature.

The NI-9227 is C-series current input module. It provides high-accuracy measurements of ±0.01% and has 24-bit ADC with 4 analogue input channels. This module not only measures the current but also the power when it is used in conjunction with voltage input module [72].

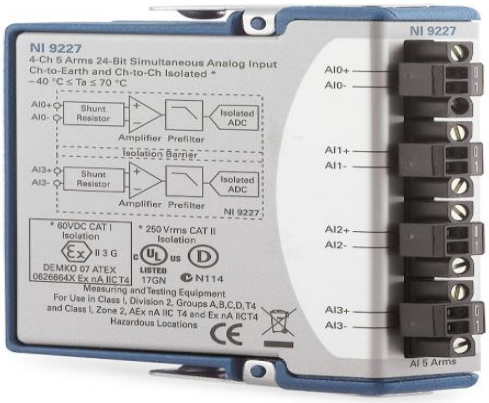

Figure 9: The module NI-9227 to measure current.

The NI-9221 is a C-series voltage input module. It has 8 channels and -60 V – 60 V measurement range. It is suitable for industrial level or small cell batteries measurements due to the wider voltage measurement range. It has a measurement accuracy of ±0.25% [73].

Figure 10: The module NI-9221 to measure voltages.

3.2.2 Data logging system

Laboratory Virtual Instrument Engineering Workbench (LabVIEW) is created by the ‘‘National Instruments’’. In this research, LabVIEW is used as data logging software to measure the temperature, voltage and current interfaced with the DAQ system. LabView is graphical programming created virtual instrument (VI). It has in-built support for NI Compact-DAQ, with several device-specific blocks for such hardware.

LabVIEW consists mainly of a block diagram, a front and a connector panel. The user interface is constructed in front panels using indicators and controls. Controls are inputs that allow the user to feed information to the program while indicators are outputs that show the results based on the program inputs. The block diagram is the program window and it contains the graphical source code on which the software engineer constructed the program by associating distinctive function blocks by illustration wires and change the properties. All items on the front panel show up as terminals in the block diagram [74]. A desktop computer system with installed LabVIEW software used to log the experimental data for the current research work.

3.2.3 Weather station

A weather station (Davis Vantage Pro2) with a temperature accuracy of 0.5°C and wind speed accuracy of ±5% was installed to measure ambient temperature (T_{amb})and wind speed (ϑ_w) and other parameters as depicted in Figure 11. It mainly comprises with rain collector, temperature sensor, humidity sensors and anemometer; radiation sensor and UV sensor can also be coupled with it. It includes the console, integrated sensor suite and mounting hardware. The specifications of the weather station are shown in the table below [75].

Figure 11: Davis Vantage Pro2 weather station.

Table 2: The specifications of the Davis Vantage Pro2 weather station.

Specifications	
Product Type	Davis Vantage Pro2
Dew point range	-76°C - 54°C
Rainfall range	0 - 99.99 in
Rainfall accuracy	±4%
Temp range	-40°C - 65°C
Dew point accuracy	± 1.5°C
Wind speed range	3 - 241 km/hr
Wind speed accuracy	±5%
Display	LCD
Dimensions	Display console: 9.5 in W x 6 in H x 1.5 in D
	Assembly: 8.2 in W x 7.25 in H x 7.75 in D
Power	110 VAC

3.2.4 Pyranometers

The analogue sensor (pyranometer) SP-110 is self-powered with an output of 0-400 mV. These are used to measure shortwave radiations for different weather networks and to optimize photovoltaic systems. Three self-powered Pyranometer with 0.20 mV per Wm^{-2} sensitivity and ±5% calibration uncertainty [20] was installed at the site (24.9°-N - 55.5° E) to measure global solar radiation intensity (G) falling on each module's surface. Pyranometers placed at the latitude angle at the upper side of PV panels so that they can directly face the sun to measure the exact radiation falling on the PV [76].

Figure 12: Self-powered pyranometer to measure the solar radiations.

Table 3: Self-powered pyranometer properties.

Parameter	**Value**	**Unit**
Power Supply	Self-powered	
Sensitivity	0.2	mV per Wm^{-2}
Calibration Factor	5	Wm^{-2} per mV
Calibration Uncertainty	± 5	%
Calibrated Output Range	0 - 400	mV
Measurement Repeatability	<1	p.p
Non-stability	< 2	p.p per year
Non-linearity	< 1	%
Response Time	< 1	ms
Field of View	180	˚
Spectral Range	360 - 1120	nm
Directional Response	± 5	%
Temperature Response	0.04 ± 0.04	% per ˚C
Operating Environment	-40˚C - 70˚C	˚C
Dimensions	24 D, 33 H	mm
Mass	90	g
Warranty	4	years

3.2.5 Thermocouples

Copper-Constanton K-type Thermocouples with an in house welded junction are deployed in this research. It has two wires, each made of different material that welded with each other at the junction and produced a voltage difference when the junction side experience the different temperature [77].

Figure 13: Thermocouples.

The K-type thermocouples used during the experimentation can measure within a temperature range of -75°C to 250°C temperature. The thermocouples are placed at different locations to measure the transient temperature distribution [78]. Calibration is the process of setting up an instrument to provide an acceptable result (within a suitable range of errors) for a sample. Accuracy is an imperative part of each analysis to trust and finish up a test result. The procedure for calibration of the instrument varies from device to device but can be defined mainly as a comparison between one known measurement of a device with another measurement made by another device in a similar way [79].

In this research, thermocouples are calibrated by measuring known temperature which is ice melting temperature T_{ice} = 0°C. The values are found close to the reference temperatures with error range 0.5°C. Also, the temperature values found by the used thermocouples are compared with a calibrated thermometer that confirmed the same measurement accuracy. The specifications of used thermocouples are listed below in Table 4.

Table 4: The specifications of used thermocouples.

Attribute	**Value**
Type	K
Number of cores	1
Core strands	1/0.2 mm
Length	25m
Minimum operating temperature	-75°C
Maximum operating temperature	+250°C
Insulation material	PTFE
Cable shape	Twin twisted

3.3 Cooling and ventilation system

This system consists of the elements that are used to construct the device to generate the atmospheric water to diminish the dust base PV losses. It consists of the following components:

- Peltier cooler
- Aluminium heat sink
- Fan
- Cooling pads
- Binding layer (Thermal grease)
- Power supply

3.3.1 Thermoelectric cooler module

The heating and cooling thermal power are generated by Thermoelectric Peltier when linked to the DC power source. The Peltier modules include two external plates made of different materials, parted by semiconductor pellets. Whenever DC current passes through the semiconductor pellets, one plate becomes cooler by absorbing the heat and other becomes hotter by dissipating the heat [80].

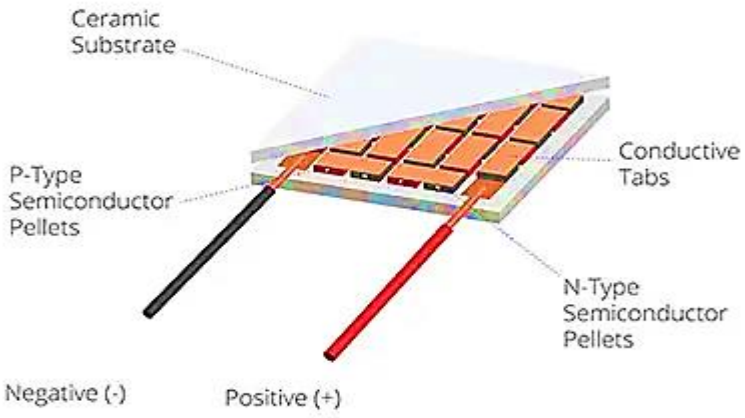

Figure 14: Thermoelectric Peltier cooler.

In this research, TEC1-12708 Peltier cooler was used as an active part for atmospheric water generation system. The specifications of the used TEC described in Table 5 [81].

Table 5: Specifications of Thermoelectric Peltier cooler.

Specifications:	
Model	TEC1-12708
Working temperature	- 40°C ~ 90°C
The maximum temperature differences	8A
Maximum refrigeration power	87.5 W
Maximum working voltage	15.4 V
Maximum temperature	75 Cel
Rated voltage	12 V
Rated current	8 A
Size	40 X 40 X 4 (L*W*H) mm

3.3.2 Heat sink

To dissipate the heat from the hotter side of the Peltier module, heat sink fabricated from aluminium having six heat pipes fabricated from copper was used during the experimentation. Peltier cooler transfers thermal energy from one side to the other through the heat sink to work effectively as shown in Figure 15 [82].

Figure 15: Heat sink.

3.3.3 Forced ventilation system

Two DC fans with dimensions (L 92 x W 92 x H 25) were used to remove the heat and cool air from the heat sinks and duct. Figure 16 shows the fan that used during the experiment.

Figure 16: DC fan used for ventilation.

It is powered by direct current (DC), operated at 12 V and rotates in one direction. The fan produces an airflow rate of 38.12 cubic feet per minute (CFM) at a rotational speed of 2000+10% revolutions per minute (RPM) [83]. Among the advantages of DC fans, they are generally extremely quiet, consume less energy and are in the economical price range.

3.3.4 Cooling pads

The 5 mm flute size pads of UltraCool 5090 are capable of good water absorption, thus providing significant cooling. It is brown available. To make these cooling pad, cellulose corrugated paper attached in an opposite sequence, which generates the space to pass the air as shown in Figure 17. The paper sheets of cellulose craft paper have an extremely high-water absorption ability, and each paper is treated chemically to prevent disintegration.

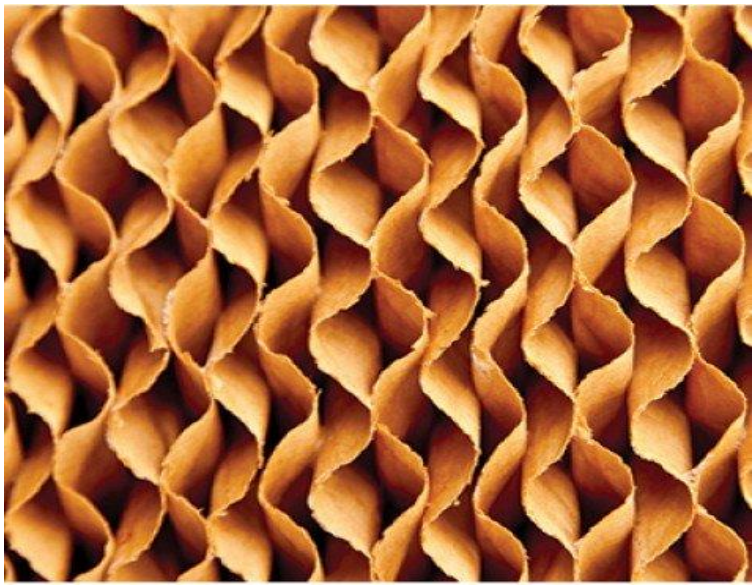

Figure 17: Honeycomb structured cooling pads.

When used in a cooling system UltraCool cooling pads are energy saving, ecologically friendly and economical because they reduce temperature without gas emissions and minimize energy costs [84].

3.3.5 Binding layer

Thermal grease HY-710 is used as interface material between the heat sink and Peltier to Thermal grease HY-710 is used as interface material between the heat sink and Peltier to reduce the interface contact resistance. It indicates a very low contact thermal resistance and a very high catalogue thermal conductivity of >3.7 W/m-K. It comprises of 30% of silicon compound 20% of carbon compound and 50% of metal oxide compounds. Silver AGO and silver powder are high cooling materials, which are included in HY710 silver thermal grease to increase thermal conductivity. It is better for CPU / GPU cooler and other electric components than regular types.

Figure 18: Thermal grease.

Thermal grease properties are tabulated in Table 6 [85].

Table 6: Thermal grease properties.

Items	**HY710**	**Unit**
Colour	Silver	No
Thermal Conductivity	＞3.17	W/m-K
Thermal Impedance	＜0.067	°C-in²/W
Specific Gravity	＞2.4	g/cm³
Viscosity	1000	No
Thixotropic Index	380±10	1/10 mm
Moment Bore Temperature	-50 ~ 280	°C
Operation Temperature	-30 ~ 240	°C

3.3.6 Power supply

The power supply is an electric device that is used to supply power to the electrical devices. A 12V DC Power Supply (S-250-12) used during the experimentation as a backup of power source for the water generation system.

Figure 19: 12V DC power supply S-250-12.

The main function of the DC power supply is to take power from an AC source and convert it into fixed DC. The AC input range may be selected by the integrated switch and it has overvoltage short circuit and overload protection system. This is made of high impurity aluminium and there is builtin DC fan for forced air-cooling to maintain the temperature [86].

Table 7: Properties of 12V DC power supply S-250-12.

Parameter	**Value**	**Unit**
Dimension	L 223 x W 68 x H40	mm
Output Current	20	A
Output Power	250	W
Voltage Accuracy	±15	%
Input (AC)	220	V
Output frequency	50/60	Hz
Working Temperature:	-10 - +60	°C
Storage Temperature	-20 - +80	°C
Ambient Humidity	20 ~ 95	%

Chapter 4: PV cleaning frequency measurement

This chapter includes the overview of the cleaning frequency and its dependencies on different factors, experimental setup & methodology, execution of the experiment and detailed analysis of the results to measure the cleaning frequency of PV panels.

4.1 PV cleaning overview

PV Cleaning has become an important subject for PV plant developers and operators as most of the PV plants are being installed in a desert area (due to the availability of space) and the margin of error is being shrunk to develop the technology up to an extent. Dust, pollution, bird droppings and shading are the main causes to render the panel less efficient [87]. A dusty PV panel is shown in Figure 20 [88].

Figure 20: Dusty photovoltaic panel.

A PV system is most effective with fully unhindered access to sunlight. Even something that is insignificant as a residual layer can affect the PV performance. Whereas larger spots, shading and obstructions can have a far greater effect than their size [89].

4.1.1 Cleaning frequency

Broadly speaking, the PV cleaning frequency depends upon five factors [90]:

- ‘‘*Location”* of the installed system that generally looks across frequent, seldom or seasonal rainfall and/or sandstorm.
- *‘‘Tilt angle’’* of the modules. The inclined panels tend to be much cleaner than horizontal.
- *‘‘Windblown dust quantity’’* is an important factor to affecting the required frequency of cleaning.
- *“Energy tariffs*” as it would justify the additional cost of PV cleaning with the financial return of additional power produced.
- *‘‘Cleaning overheads’’* such as water consumption and infrastructure modules required for cleaning.

4.2 Experimental procedure to determine cleaning frequency

An approach to analyse and quantify the effect of dust on solar radiation penetration and PV modules performance has been undertaken and appropriate time span for PV cleaning has been determined in the research. In this work, radiation losses resulting from the accumulation of dust on the surface of the PV module are measured. The experiment has been carried out at the ‘‘Renewable Energy Laboratory’’ Falaj Hazza Campus, United Arab Emirates University, Al Ain, United Arab Emirates. The site is situated at latitude and Longitude of 24.9° N - 55.5° E respectively. The campus is located between a residential and an industrial area surrounded by some date palm trees. Near the building is a road with high traffic flows that may further enhance the airborne particles.

Four arrays each containing six monocrystalline photovoltaic modules with dimensions of 99 cm x 134 cm, rated capacity of 160 W were installed at the site as shown in the figure. The modules electrical performance has been confirmed by measuring V_{OC} and I_{SC} prior to dusting study.

Figure 21: Photovoltaic modules array installed at UAE University, Falaj Hazza Campus.

To measure the pure radiations losses caused by the dust, four transparent glasses with 3 mm thickness used in this research to mimic the top glass cover of the PV modules understudy. Four self-powered SP-110 Pyranometers were installed at the back sides of transparent glasses, and one is installed at the latitude angle at the front side of glass modules to measure solar radiation intensity (G) falling on each module's surface before and after the transmission through the glass. One of the reference glass modules has been cleaned on a daily basis, while the other four has been cleaned after 10 days, 20 days, 30 days and 3 months representing a seasonal scale respectively. Meanwhile, the pyranometers also placed at the latitude angle at the top side of PV panels, so that they can directly face the sun to obtain the maximum radiations.

In order to measure the value of irradiance, the voltage obtained by the pyranometers using NI modules needs to multiply with a constant (5000) which is provided by the pyranometer manufacturers. Other parameters, such as temperature, rainfall, wind speed and humidity have also been measured by using the ‘’ Davis Vantage Pro2’’ weather station as shown in Figure 22.

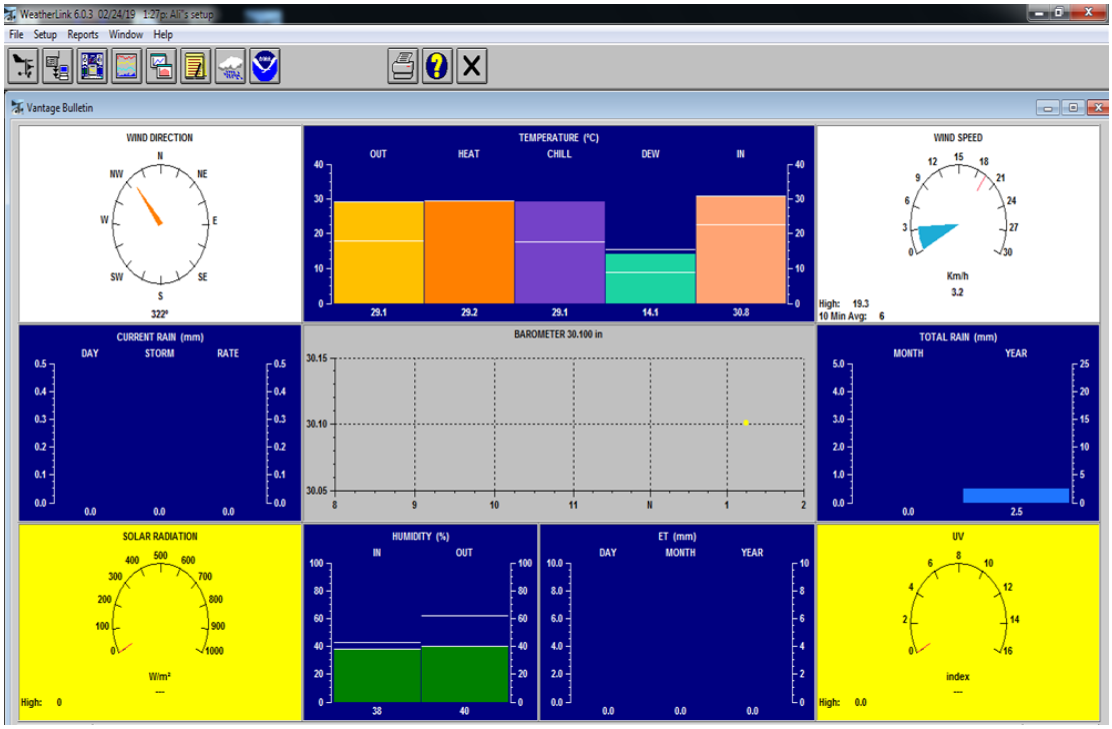

Figure 22: Weather station software user interface.

The measurement uncertainties for all the devices are listed in Table 1.

Table 8: The measurement uncertainties for all used devices.

Parameter	**Device**	**Model**	**Measurement range**	**Accuracy**
Solar radiation	Apogee Pyranometer [76]	SP – 110	-	±1%
Data acquisition	NI-Compact DAQ [70]	9178	-	±0.02%
Current	NI-Analogue module [72]	9227	-5 A – 5 A	±0.01%
Voltage	NI-Analogue module [73]	9221	-60 V - 60 V	±0.25%
Temperature	Ni-Analogue module [71]	9213	-75°C - 250°C	±1%
	Thermocouple K-type [78]	363-0389	-75°C - 250°C	±1.5 (°C)
Ambient temperature	Davis vintage pro2 weather station [75]	6152	-40°C to 65°C	±0.5°C
Wind speed	Davis vintage pro2 weather station [75]	6152	1 to 67 ms^{-1}	±0.5°C

All the sensors and the power output cables from the PV modules were connected to a NI-Compact DAQ through current and voltage modules to log the data as shown in the schematic of the experimental setup in Figure 23.

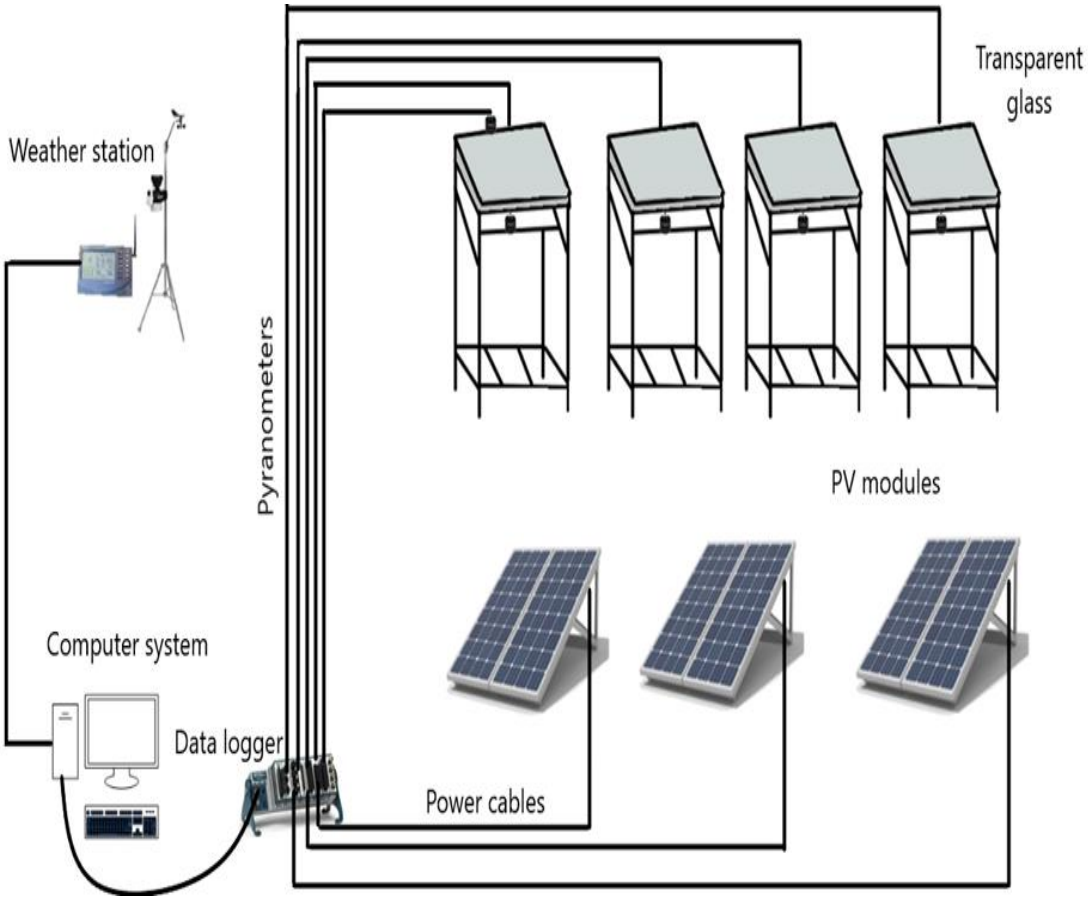

Figure 23: Schematic diagram to measure the power and radiations losses due to dust to determine the optimal cleaning frequency of PV modules.

By comparing recorded irradiance values measured by the pyranometer that is installed beneath the reference glass module (which gets clean daily manually by using water and wiper) with the other pyranometer values that installed below the other modules (which get cleaned after 10 days, 20 days, 30 days and seasonal basis), dust influence on the received radiation can be quantified, and as a result its effects on the

solar radiations received by these pyranometers. Similarly, the power losses caused by dust are determined by comparing the measured voltage and current by NI modules of the cleaned and the dusty PV panels. Front panel window and block diagrams codes used in this study are shown in Figures 24 and 25 respectively.

The front panel is a window for the user to monitor and manage the program. The temperatures, voltages and currents are measured in Celsius, volts and ampere respectively. The time delay can be set manually, and the program can also be started & stopped manually as shown in Figure 24.

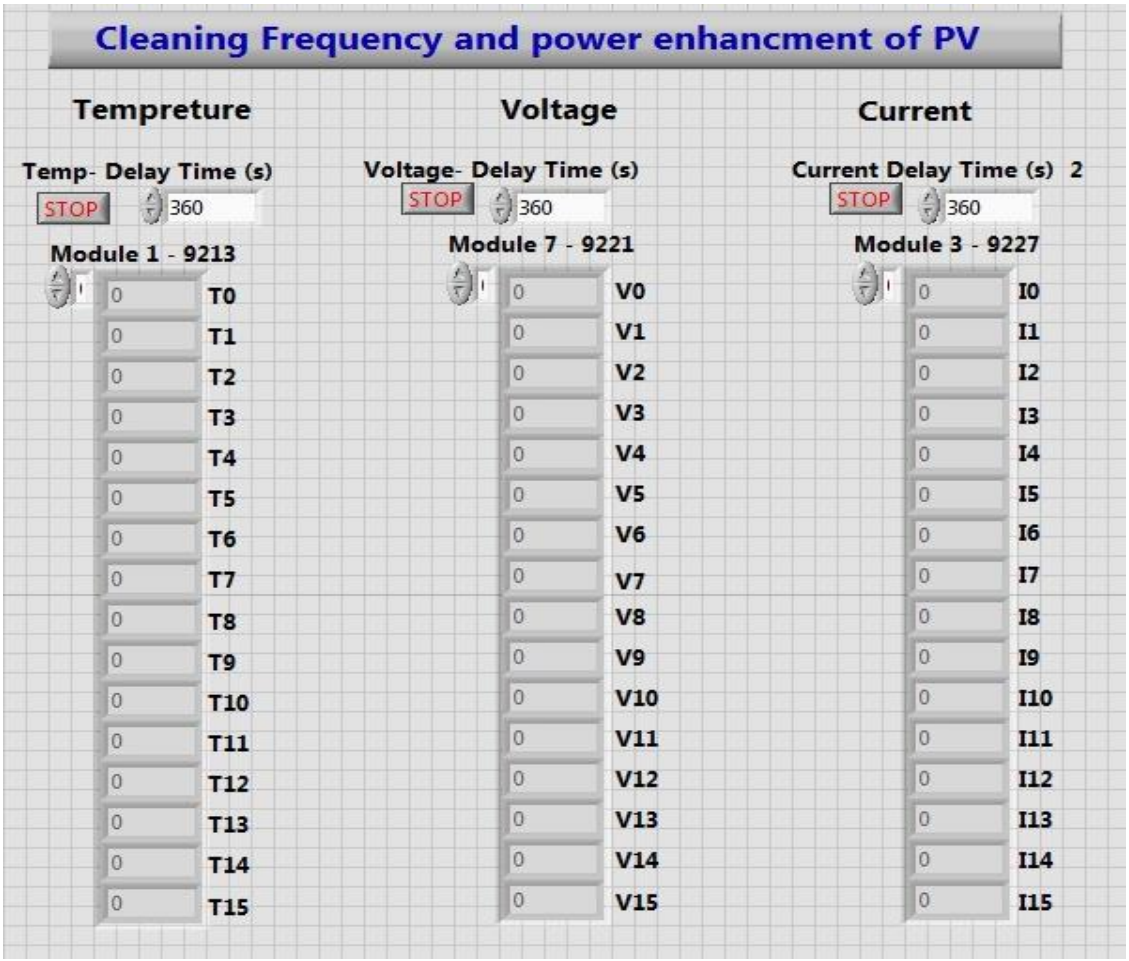

Figure 24: The front panel window of the LabVIEW program to measure voltage, current and temperature.

The block diagram as shown in Figure 25 is a working window where the program is prepared. The system is connected to the Excel program to record the data tables for further analysis.

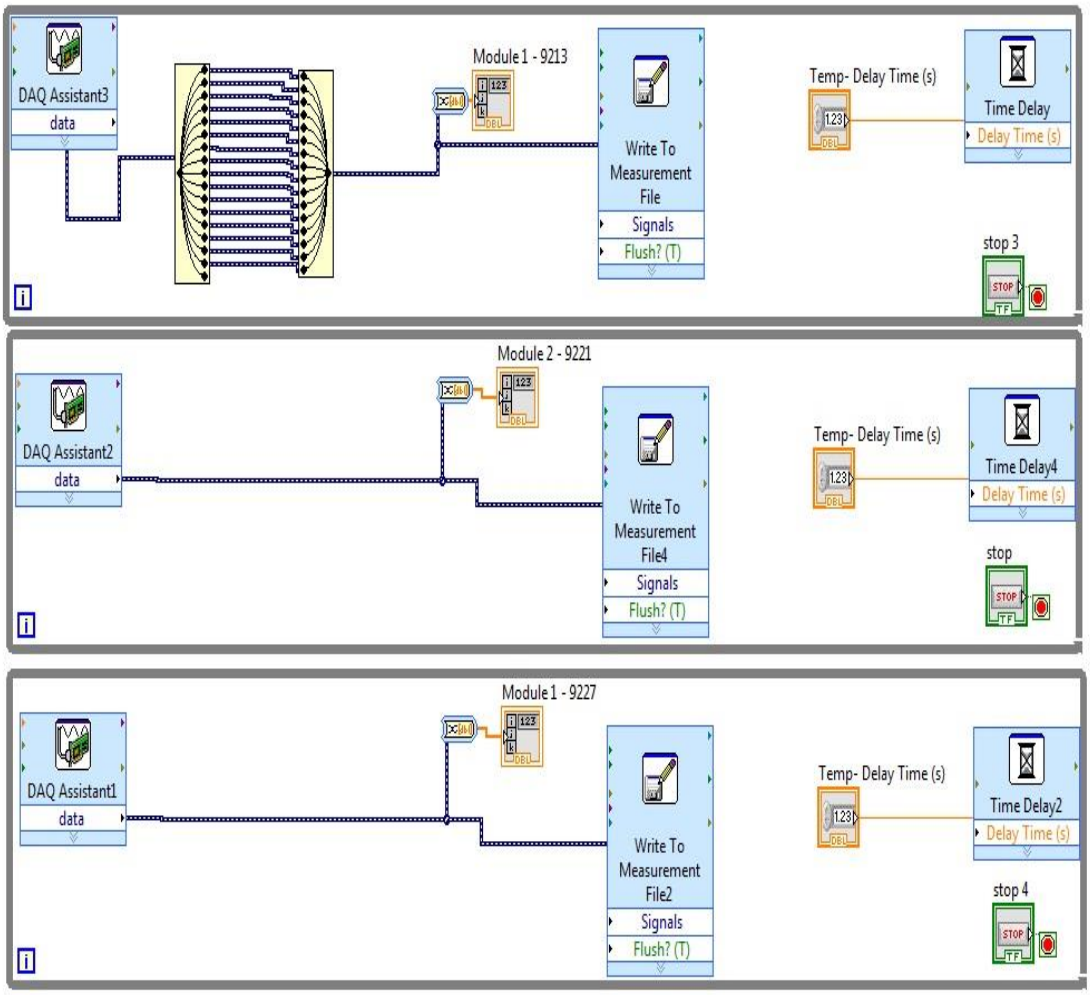

Figure 25: Block diagram of the LabVIEW program to measure voltage, current and temperature.

The experiments were conducted for almost three and a half months from 22/04/2018 to 07/08/2018 start at 06:30 AM and end at 06:30 PM. The data was logged for all systems with a time step of 5 minutes. The weather remained dry without any rain during this period.

4.3 Experimental results and discussion

The experimental results were obtained and recorded at the end of 10 days, 20 days, 30 days and three months. The results to measure the cleaning frequency are described below with figures in details.

4.3.1 Weather data

Figures 26 show the ambient temperature (T_{amb}) and wind speed (ϑ_w) for the duration of the experiment. It shows the weather data for the first 10 days that average daily T_{amb} increased from 27.3°C to 34.2°C peak in the afternoon time. The average wind speed (ϑ_w) remained lower than 2.2 m/s with an absolute average value of 1.7 m/s during the tested period.

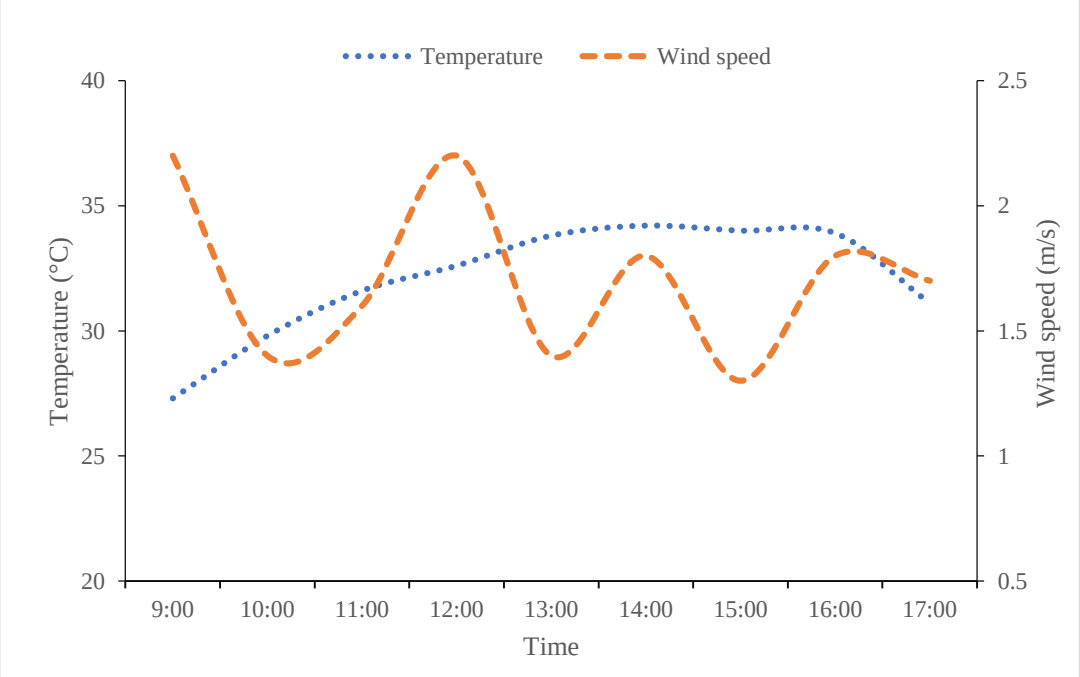

Figure 26: The weather data for the first 10 days of experiments.

For 20 days of experiment the wind speed (Vw) again remained low with an average peak and absolute average values of 2.6 m/s and 1.97 m/s respectively as shown in Figure 27. The ambient temperature reached its maximum value of 38.8°C at mid of the day.

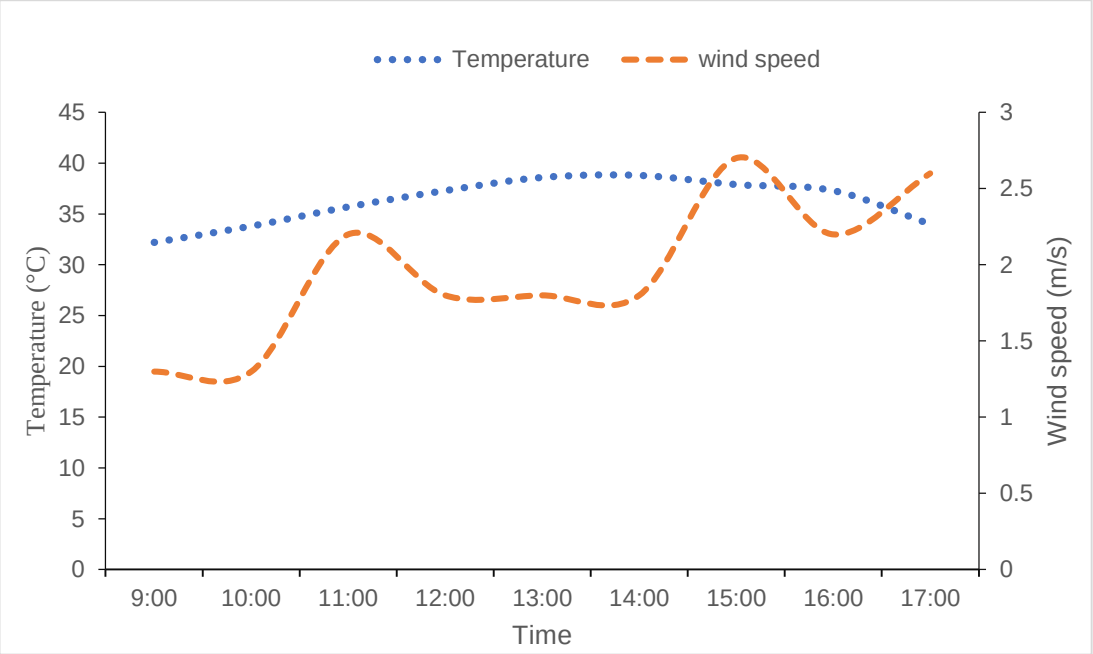

Figure 27: The weather data for the first 20 days of experiments.

The weather data values for one month and three months depict the high ambient temperature between the range 34.6°C to 44.6°C and 38°C to 46.8°C respectively. The wind speed shows with a substantially higher value with the average speed of 7.35 m/s for both testing duration but with the different peaks as shown in Figures 28 & 29 below.

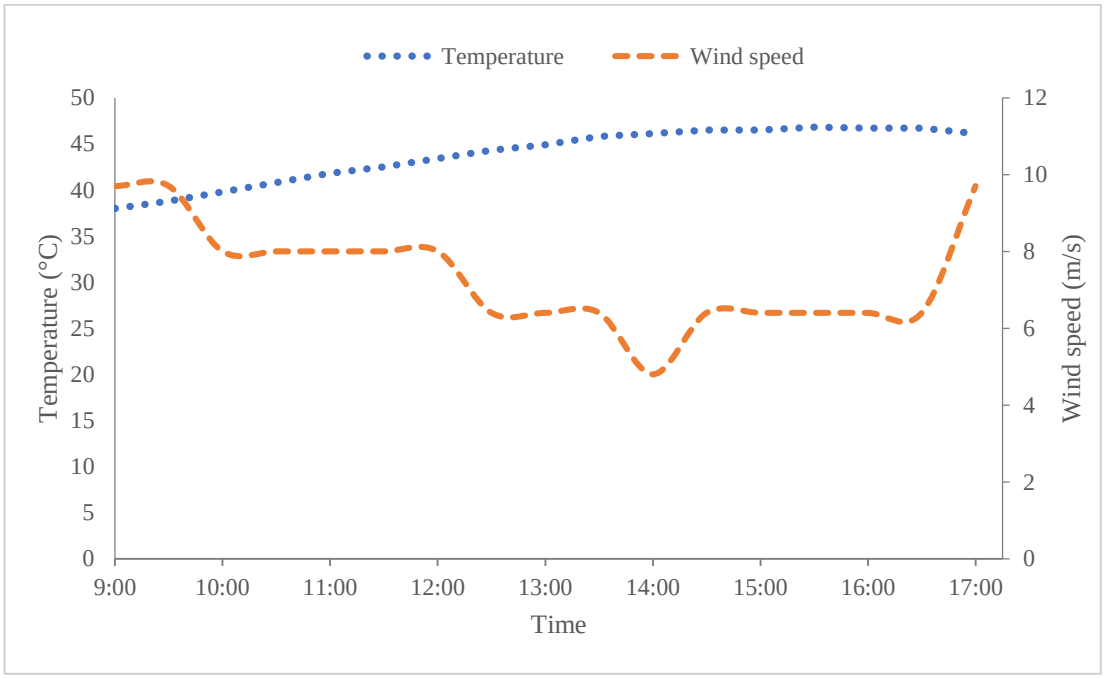

Figure 28: The measured weather data for one month.

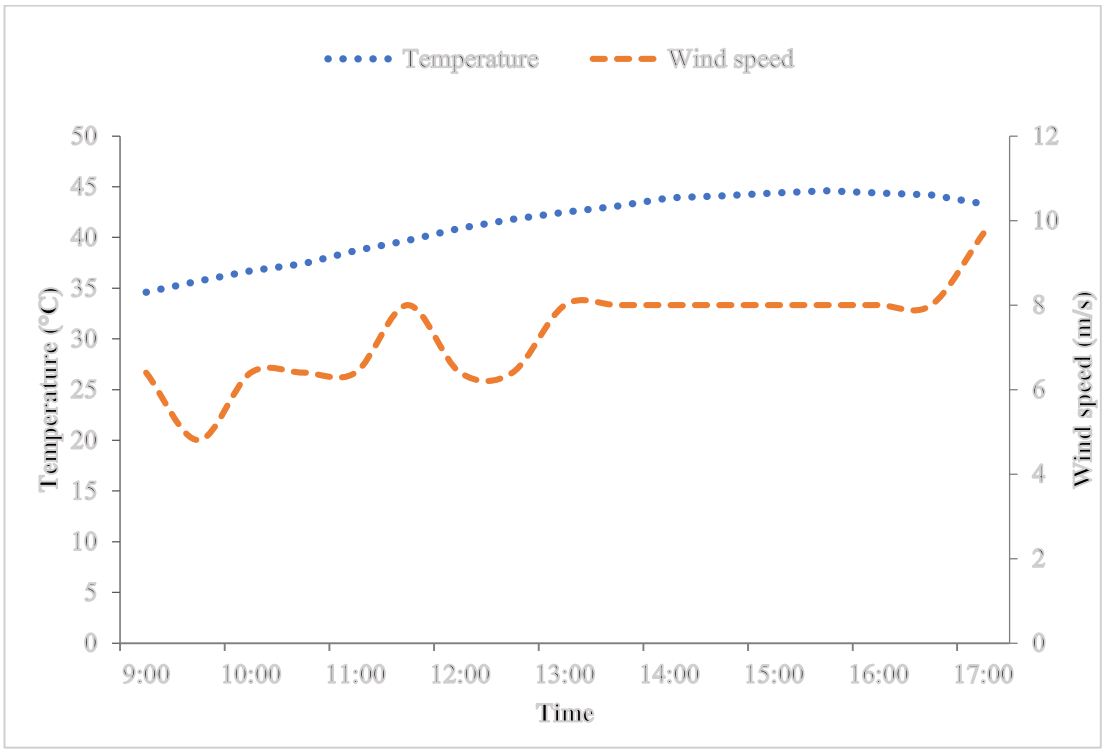

Figure 29: The measured weather data for 3 months.

Air circulation around the PV surface due to windy conditions causes the loss of heat by natural convection, which is empirically predicted by [91]. In the case of a PV module in air, Eq. 1 provides the complete exchange of convective energy from a module's surface. At 45° wind incidence angle, the wind-induced convective heat transfer coefficient (h_c) is given by Eq. 3 [92].

$$q_{conv} = -(h_c) \times A \times (T_{PV} - T_{amb}) \quad \text{(Eq. 2)}$$

$$h_c = 9.5\vartheta_w^{0.46} \quad \text{(Eq. 3)}$$

The lower h_c values show that natural convection cannot efficiently cool the PV, which leads to higher PV temperatures that eventually affects the PV electrical conversion efficiency. However, lower h_c values can be potentially beneficial once the concept of thermal energy storage and recovery is introduced in the PV, as it would minimize heat losses.

4.3.2 Radiation losses due to dust

Solar radiations that are absorbed by the PV ($Q_{absorbed}$) depends on the surface area (A) and the dusting coefficient (d_c) which represents the PV surface cleanliness and the absorptance (α) of the PV panel as given by Eq. 4.

$$Q_{absorbed} = G \times A \times d_c \times \alpha \quad \text{(Eq. 4)}$$

Figure 30 shows the incident solar radiation on static glass surfaces and the reduction in solar radiation penetration into the surface due to the deposited dust layer on the front glass surface with the passage of time. The global radiations incident at the surface of the glass and their value after the penetration from glass modules cleaned daily after 10 days are shown in Figure 30. The data is recorded prior to cleaning the modules.

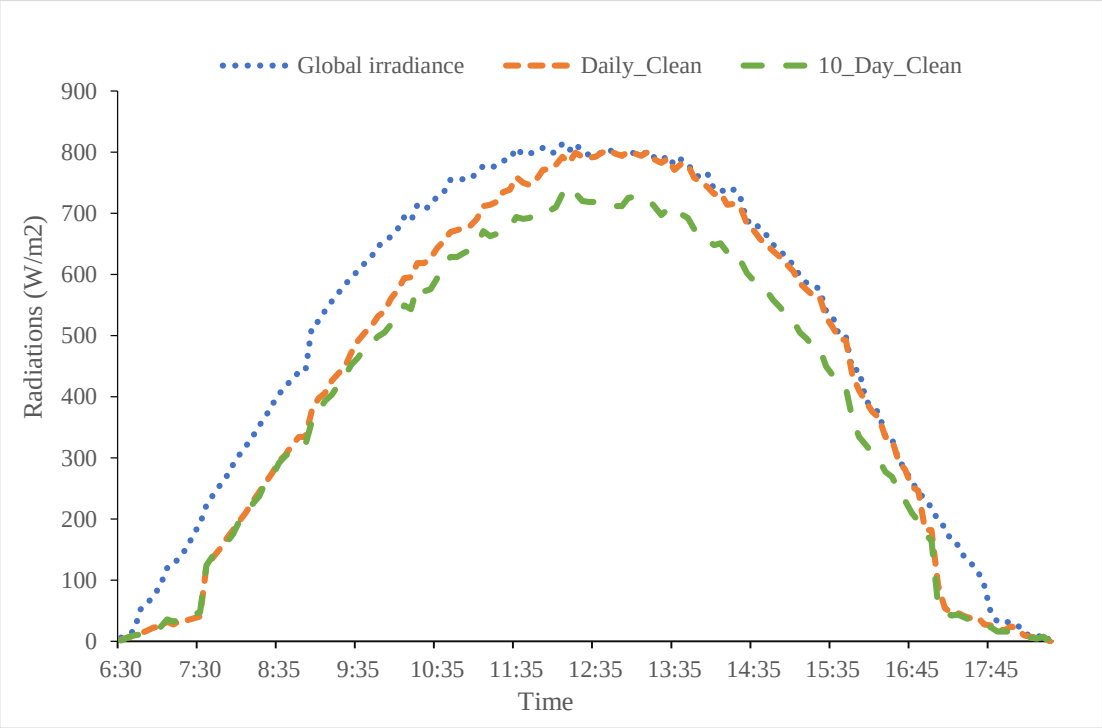

Figure 30: Global radiation, radiation after passing through the daily cleaned glass module and the radiation after passing through the glass module cleaned for 10 days.

There are the average and peak radiation drop of 43 W/m^2 and 87 W/m^2 was recorded between the daily cleaned glass module and the 10 days dusted glass module as shown in Figure 30.

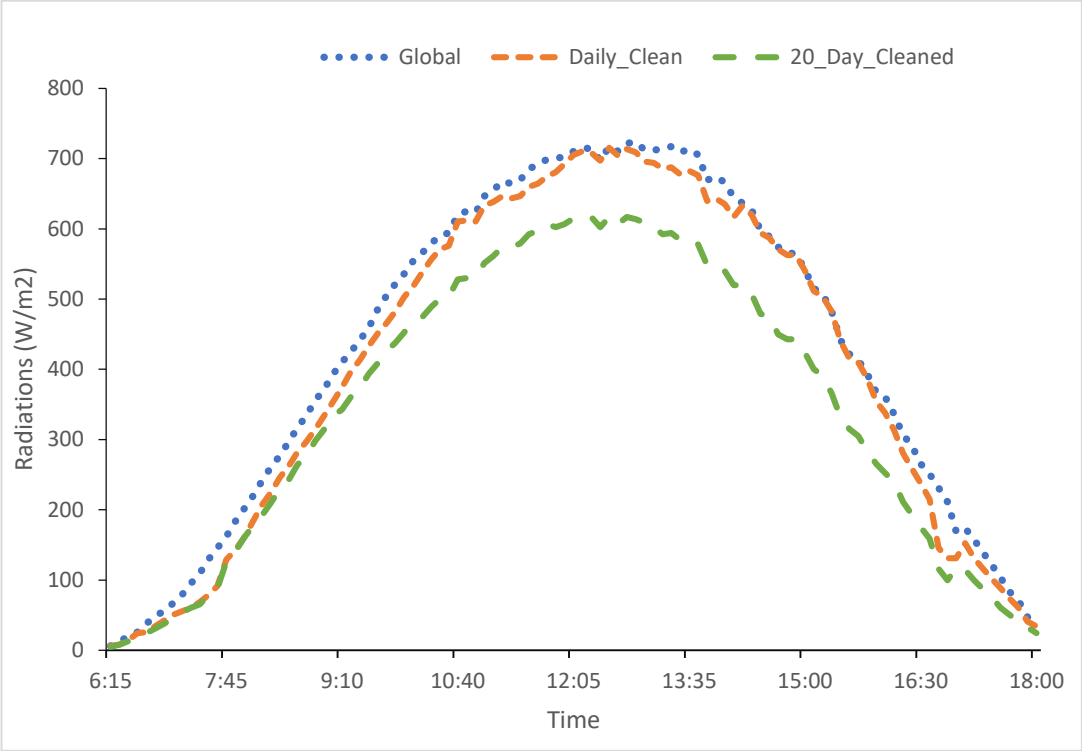

Figure 31: Global radiation, radiation after passing through the daily cleaned glass module and the radiation after passing through the glass module cleaned after 20 days.

The amount of solar radiation transmission through the glass is decreasing as the amount of dust kept increasing at the module surface. The average and peak radiation transmission difference through the glass module reach up to 57 W/m^2 and 118 W/m^2 for the daily clean glass module and the glass module cleaned after 20 days.

The radiation transmission for monthly cleaned glass module decreases up to almost 19% with respect to the daily cleaned glass module. It was noted that the peak radiation drop was 120 W/m^2 and the average radiation drop was 65 W/m^2.

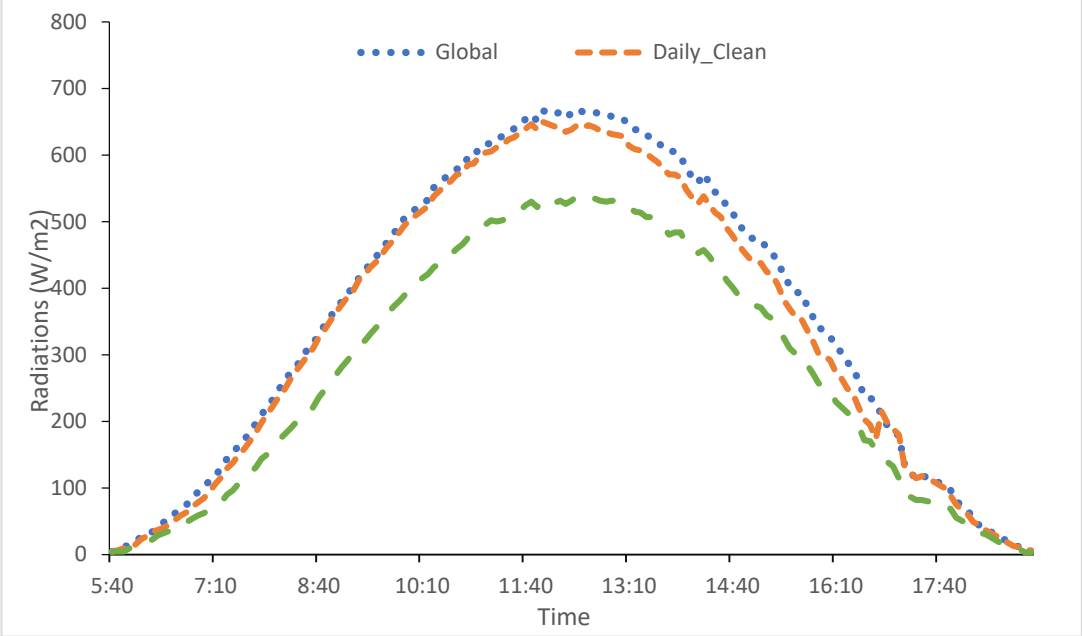

Figure 32: Global radiation, radiation after passing through the daily cleaned glass module and through the glass module which did not get cleaned for a month.

Figure 33 shows the radiation loss in a PV module kept dusted for 3 months compared to a daily cleaned module. The peak and average drop of radiation for 3 months dust accumulation was 239 W/m^2 and 118 W/m^2 respectively reaching up to 27% loss during at peak time.

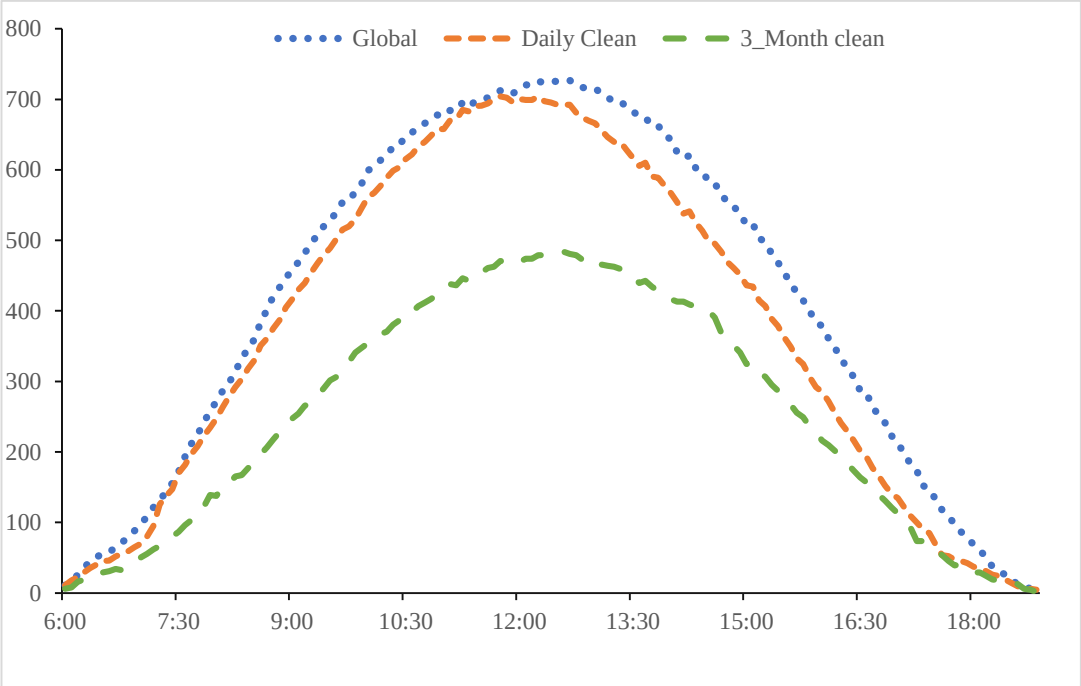

Figure 33: Global radiation, radiation after passing through the daily cleaned glass module and through the glass module which did not get cleaned for 3 months.

Table 9 summarises the global radiations after days of dusting, average radiation after the transmission through specific glass modules and the loss of average and peak radiations that passes through the glass modules with different level of dust accumulated at their surface. Here, C_d shows daily cleaned glass module, C_{10_d} shows the module dusted for 10 days, C_{20_d} depicts the module dusted for 20 days, C_m and C_{3_m} shows the modules dusted for a month and 3 months respectively.

Table 9: Radiation level for glass modules, accumulating with different level of dust

Period	**Global radiation**	**Average radiation**	**Average difference**	**Peak difference**
C_d	497	446	43	87
C_{10_d}	497	403	43	87
C_d	407	386	57	118
C_{20_d}	407	329	57	118
C_d	360	343	65	120
C_m	360	278	65	120
C_d	415	372	118	239
C_{3_m}	415	254	118	239

4.3.3 Power drop due to dust adhering

Several factors affect the solar panel output although the predominant ones are dust driven solar radiation losses, which reduce PV current and elevate PV operating temperature, which induces voltage loss [93]. The dust layer accumulation on the surface of PV diminishes the solar radiation penetration into solar cells which directly cause the PV power drop. When the sunlight strike at the surface of the PV module, due to the dust particles settling on PV modules the radiations get scattered and could not contribute to the power generation. The longer the exposure to the solar cell, the more dust will be accumulated on the surface and therefore the more power drop shall be expected [94].

The dust accumulation has a negative effect on current due to the less penetration of solar radiations, which causes to decrease in charge mobility. The measured V_{OC}, I_{SC} and electric power for C_d and C_{10_d} are shown in Figure 34 and 35 respectively. The peak V_{OC} was recorded as 39.8 V for $C_{10\text{-}d}$ PV compared to 39.9 V for reference Cd PV which shows a negligible voltage drop. On the contrary, the Isc for C10-d and Cd PV modules are 5.39 A and 5.5 A respectively, showing a drop of 2% in the current.

The electrical power output of all 4 PV modules is calculated from the measured electrical parameters of V_{OC} and I_{SC}, by employing the fill factor as shown in Eq. 5.

$$P = Voc * Isc * FF \quad \text{(Eq. 5)}$$

Where P is the PV generated electrical power and the FF is considered to be constant (0.74) deduced by multiplying the rated voltage V_{mpp} with rated current I_{mpp}

over V_{OC} and I_{SC} as given by Eq. 6. The V_{mpp}, I_{mpp}, V_{oc} , and I_{sc} are listed in the PV data sheet from the factory.

$$FF = \frac{V_{mpp} \times I_{mpp}}{V_{OC} \times I_{sc}} \qquad \text{(Eq. 6)}$$

In the UAE atmospheric conditions with no major sand storm, the PV lost 3% power without being cleaned for 10 days

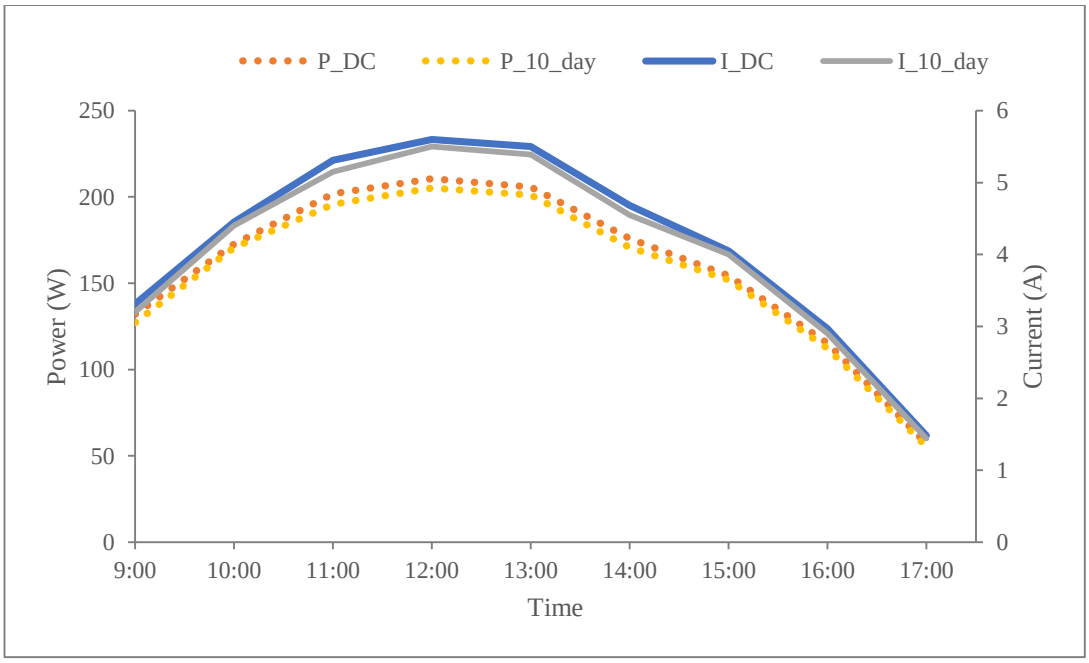

Figure 34: Current and power for the daily cleaned and 10 days dusted PV panel.

The effects of dust accumulation at the surface of PV modules for 20 days compared with the reference PV panel cleaned daily is presented in Figure 35. The peak voltages and currents for daily cleaned and Cd-20 are 38.6 V,4.99 A and 38.6 V, 4.8 A respectively as shown in figures below showing a drop of 3.9% in current with the voltage being unaffected. Similarly, the power comparison shows a 5% power loss for a PV cleaned after 20 days compared to the daily cleaned PV panel.

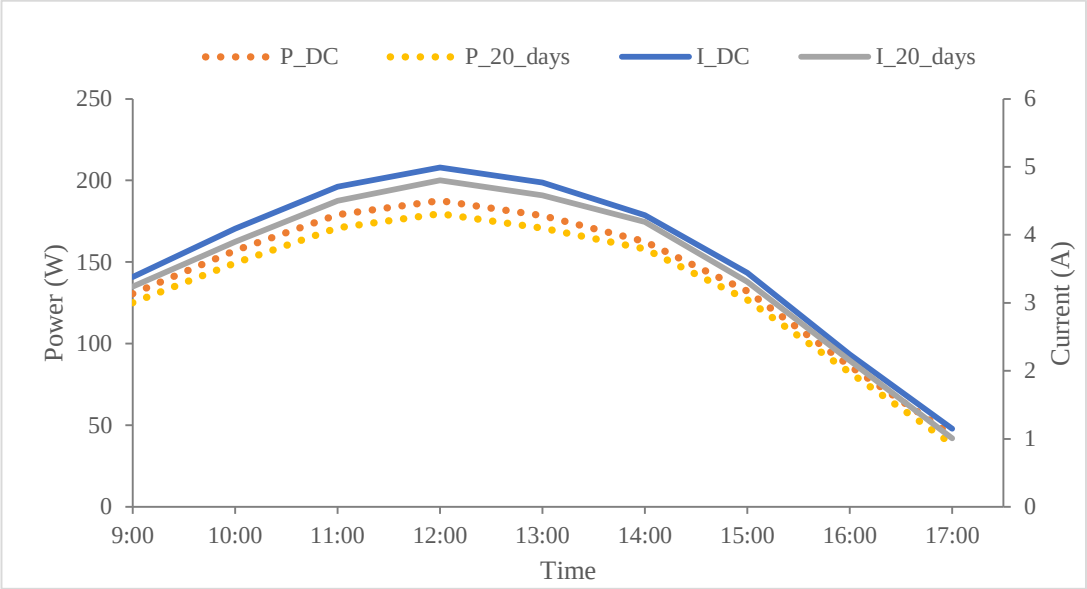

Figure 35: Current and power for the daily cleaned PV panel compared to the panel dusted for 20 days.

The current and power due to the effects of dust accumulation over the period of one month and daily cleaned PV modules are shown in Figure 36. The dusty panel for a month shows the decrease in current and power produced by the PV.

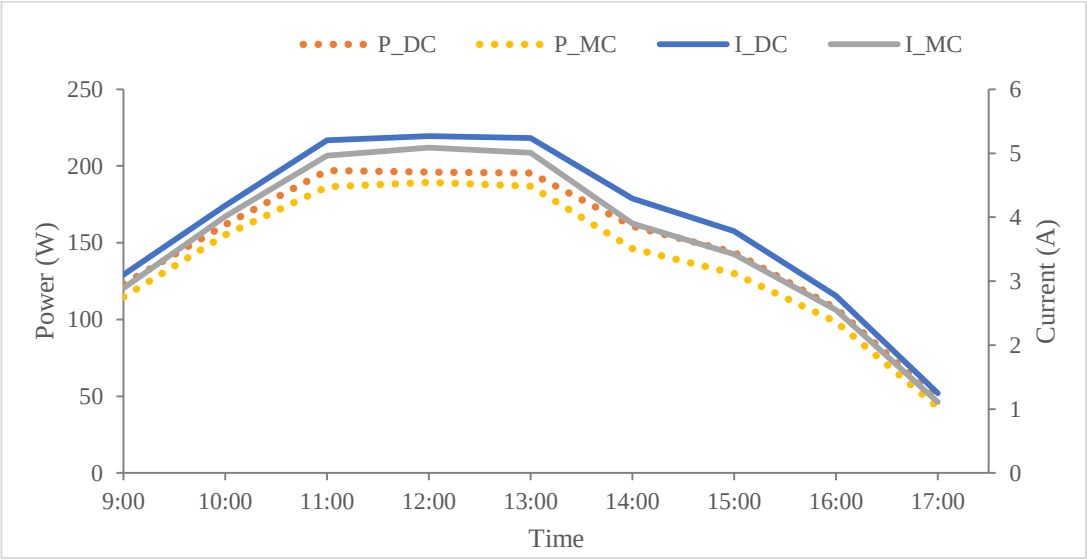

Figure 36: Comparison of current and power of the daily cleaned panel compared to the panel dusted for one month

Power comparison between the daily cleaned PV and a PV cleaned after a month shows a significant power drop of 7%. This power drop occurs due to the dust layer deployment on the surface of the PV. Surprisingly though the panel dusted for three months showed a drop in both voltage and current. The peak V_{oc} was recorded as 38.4 V for three months dusted panel compared to 39.9 V for reference daily cleaned PV. Similarly, the peak I_{sc} for daily cleaned PV modules was 4.48 A which dropped to 4.02 A for the panel cleaned after 3 months. Eventually, a similar trend was observed for the power drop for the PV module cleaned daily and after 3 months respectively as shown in Figure 37.

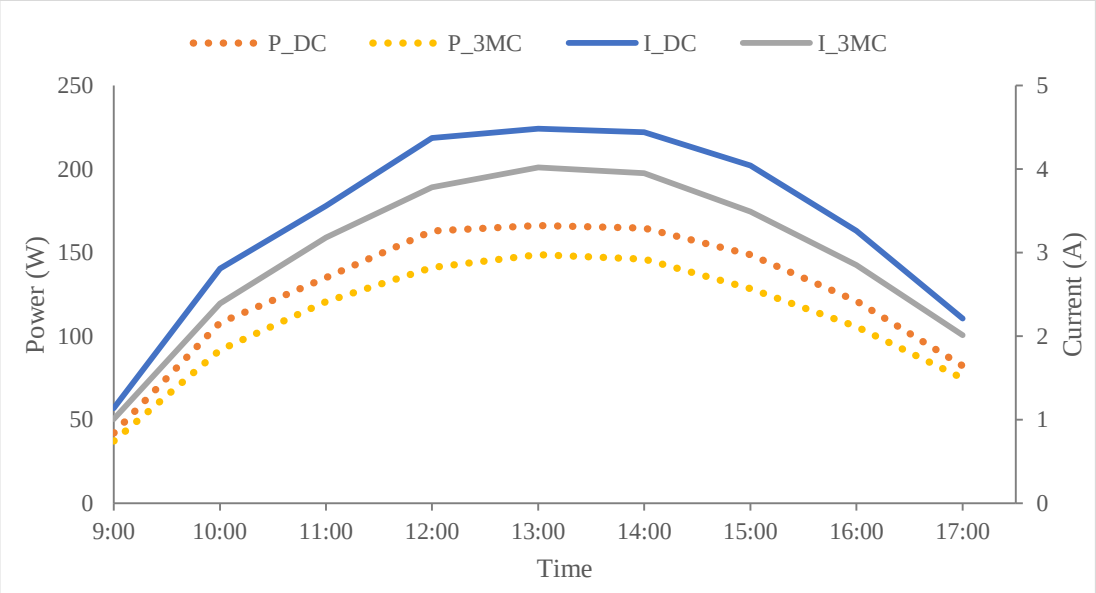

Figure 37: Current and power produced by daily cleaned PV compared to the PV cleaned after 3 months.

The average power produced by PV-Cd and PV-C_{3_m} is 110.5 W and 127 W respectively showing a 13% power loss in dusty panels for 3 months. The importance of cleaning reflects clearly from the above-described results. For example, a solar plant which produced 100 MW when it's fully cleaned, if this plant does not get clean for 3

months then there will be a 13 MW of power loss due to the dust accumulated at its surface.

Figure 38 depicts the radiation loss and power loss over time for all the cases, daily, 10 days, one month and 3 months. As it can be seen that power difference between daily cleaned PV panel and dusty PV panel for the specific period of time (10 days, 20 days, 1 month and 3 months) increasing as the radiation penetration difference increasing between daily cleaned and dusty glass module.

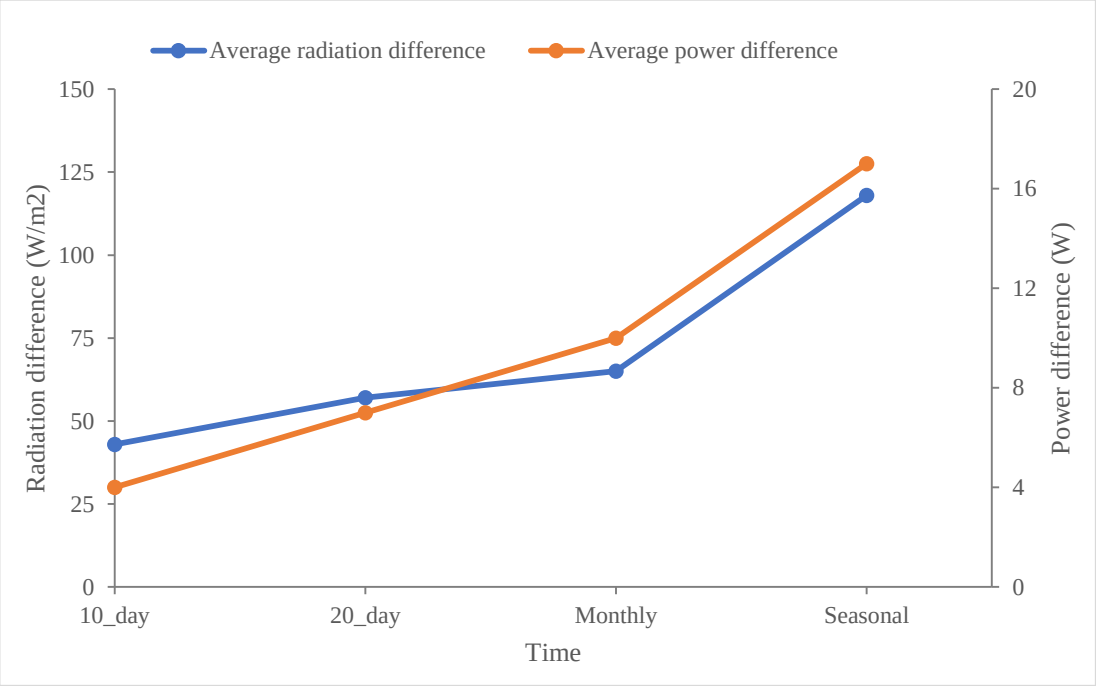

Figure 38: Power loss due to the radiation for the period of 10 days, 20 days, a month and 3 months.

Basic investigations to measure the cleaning frequency and power drop due to the dust accumulation at the surface of modules have been done at the array level. Future work concerns with in-depth study for a year at the plant scale and modelling algorithm development to validate the experimentation.

Chapter 5: An atmospheric water generation system for PV cleaning

This chapter provides the basics of the concept of atmospheric water generation. It includes the summery and design of the AWG system and how to exploit the diurnal dew point drop, radiative cooling over a sky exposed surface and Peltier cooling in sequential order to optimize the self-reliant PV cleaning system. Experimental setup, methodology and water generation results are discussed in details in this part of the study. It also described the Simulink modelling of the AWG system (to make it autonomous and self-reliant using the discarded power) with a detailed analysis of the results.

5.1 Basics and background

The most common means of cleaning PV from the dust employs water flushing over the PV panel surface. For larger scale utility PV power plants, water transportation and consumption required for PV cleaning incurs tremendous overheads on the plant operations thus increasing the electricity production cost. Besides, most of the utility-scale PV plants are installed in a desert environment that poses a two folds challenge of increased dust accumulation coupled with lack of water supply infrastructure to keep the plant cleaned. The current research proposes a solution for water production by extracting water from the air. The proposed solution can solve water transportation problems for PV cleaning in water droughted areas. The embodiment of atmospheric water generation system will exploit the diurnal dew point drop, adiabatic air expansion in porous media, radiative cooling over a sky exposed surface at night and Peltier cooling in sequential order to optimize the self-reliant PV cleaning system.

Atmospheric dew point depends upon the air pressure and humidity level and varies according to these parameters. The dew point is the temperature that is enough to saturate water vapours in the air. The airborne vapours condense into a liquid when further cooled down [95]. When the air temperature reaches up to its dew point and then strike at the surface that has a lower temperature than air, the water will adhere at that surface. The ambient temperature and the number of water vapours in the air determine the dew point temperature [96]. The objective is to achieve the saturation temperature in order to condense vapours into the water using some passive and active devices. Since the relative humidity keeps changing in time and space, a customized set up is required to assure the condensation at all conditions [97]. The hot and humid climate is very appropriate for water extraction from the air. At this stage, the air has a significant amount of vapours content that can be condensed into water by using atmospheric water generation (AWG) setup [98]. With the increase of air temperature, the water vapours carrying capacity of the air also increases, means the same volume of air has the capacity to hold more vapours, thus decreasing the chance for water production at elevated temperature. Thus an AWG system has to adopt all means to reach the right temperature that could assure condensation to produce water.

5.2 Summary of AWG system

Apparatus for the device for a PV cleaning system mainly comprise of a Peltier module, customized heat sinks to draw out the heat from one side of the Peltier, fans to draw out the air from both sides of the Peltier, diverging duct to expand the air, honeycomb structure to trap the air, voltage sensor, current sensor, temperature sensor, humidity sensor and a controller. The device is lightweight and easy to integrate at the PV module. In one embodiment, the device is mounted at the top of the PV module. In

utility-scale PV power plants, the output of the PV array through inverter has to meet the grid specifications in terms of power quality. As long as the inverter output is not compatible with the grid, the power will be injected to the proposed cooling system instead of being wasted as happens in the conventional case. Part of the power recovered through the PV will be utilized to draw cooled ambient air to the cooling unit.

At the first stage, air will be subjected to expansion through a diverging duct/nozzle to cool by adiabatic expansion. Temperature is related to the average of the square of the velocity of the molecules in a gas. The air temperature is directly proportional to the air molecules' kinetic energy. When the air gets expand through a diverging duct then due to the expansion of the air, the kinetic energy and collision of air molecules reduced, which causes to decrease the temperature of the air [99]. The surfaces of the duct will be exposed to sky to cool radiatively the surface at night and aid in air cooling. Radiative cooling is the transport of energy to the deep space, as it has a temperature close to zero, which makes outer space to behave as a heat sink [100, 101].

At a second stage, the air will be further passed through a porous structure (honeycomb) contained within a section of the duct to cool by the capillary/thermocapillary effect. At the last stage, the air will be passed through a cooling plate chilled by Peltier cooler to condense and extract water from the air.
The water will be stored in one embodiment in the voids of the porous structure which will later be wiped off the panel to clean the dust. Water in the other embodiment will be stored in a storage box and will be sprinkled over the PV surface to be wiped and cleaned. The Inventive steps in the research which distinguished it from others are that it integrates a systematic and hierarchical passive and active design to generate water from the waste energy and does not involve additional energy inputs. The second step

involves including the Peltier cooling system which consumes substantially lower energy compared to the conventional compressor-based condensation systems. The contextual relevance of the research is another step which entails producing atmospheric water in the harshest summer conditions of gulf region which renders it more interesting with its airborne dusty environment to devise such an invention.

5.3 Embodiment of the system

The experiment has been carried out at the ‘‘Renewable Energy Laboratory’’ Falaj Hazza Campus, United Arab Emirates University, Al Ain, United Arab Emirates. The site is situated at latitude and Longitude of (24.9° N - 55.5° E) respectively. The campus is located between a residential and an industrial area surrounded by some date’s trees. Near the building is a road with high traffic flows.

The copper and aluminium made heat sink with four heat pipes, used to draw out the heat from the hotter side of Peltier cooler. The heat removal from the hotter side is necessary, otherwise, the Peltier cooler will become hotter on both sides and may damage the device [82]. The hotter side of Peltier cooler was checked and confirm before attaching it with the heatsink. The aluminium based plate was attached at the cooled side of TEP. At the left end of the device, the ambient air is mechanically drawn in the divergent air duct through the DC fan, which is installed at the inlet of the duct. At the wider end of the duct, a porous structure (cooling pad) is installed to trap and furtherly cool down the air. The air temperature decreased somewhat due to the air expansion, it further decreased when passed through the radiatively cooled sky exposed air duct. Finally, this cooled air strikes at the aluminium plate attached with the cooler side of TEP to condense water vapours. The schematic diagram of the setup shown in Figure 39 below.

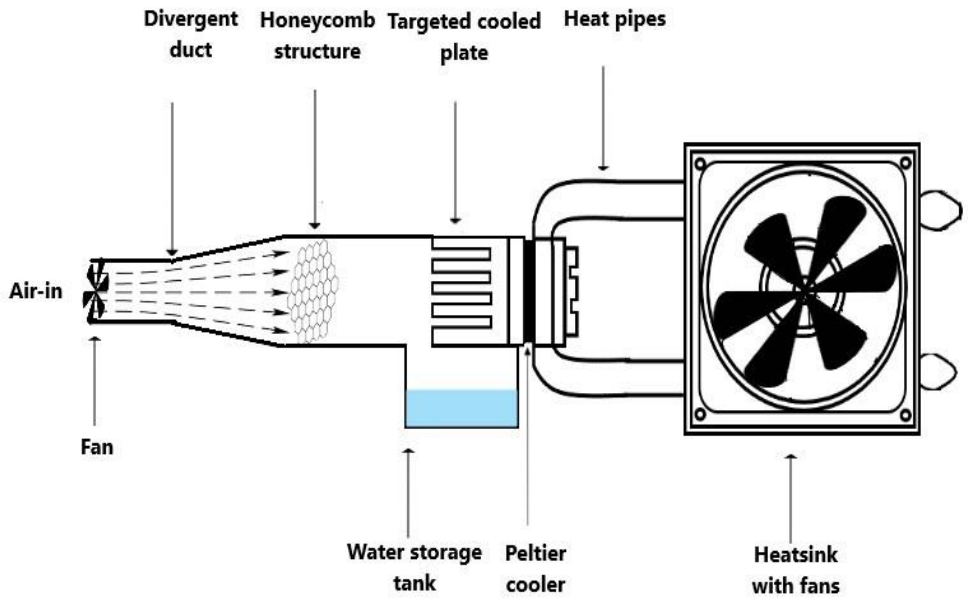

Figure 39: The schematic diagram of atmospheric water generation system.

5.4 Specification of the AWG system

Mainly the device is to produce water in a consistent way to clean the PV panels in water droughted areas by condensing the moisture in the air. The specifications of the system are listed below:

- It harvests the wasted power from PV to feed into the AWG system.
- It provides a low-cost water production system exploiting the natural phenomenon in the sequential order and injecting active power as needed.
- It is a compact and low weight water production system that can be mounted to the existing PV system.

5.5 Results and discussion

The experimental assessment of the proposed AWG was conducted for three days of device operation. The measured weather conditions and water production data are described in the following section.

5.5.1 Weather data

This section represents the trends of ambient temperature, wind speed, humidity and dew point temperature for the three different days (day & night) of the experimentation. As shown in Figure 40 at the 1st day of the experiment the humidity remained predominantly below 40% during the day time and remained predominantly above 40% during the night time for almost 14 hours from 5:30 PM to 7:30 AM.

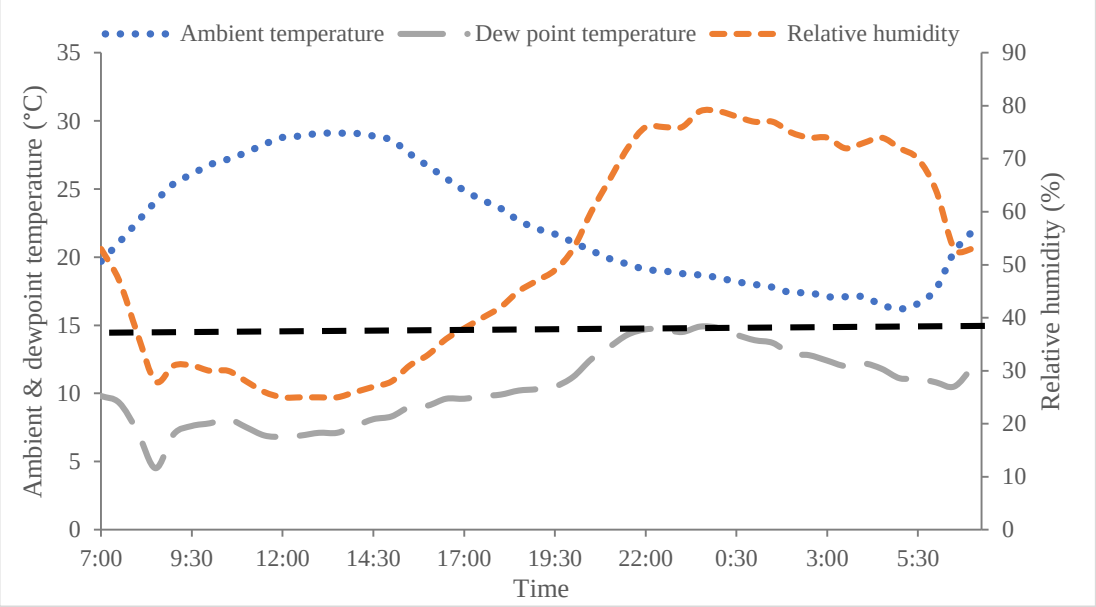

Figure 40: The measured relative humidity, ambient air temperature and dew point for the 1st day of the experiment at the site in Falaj Hazza Campus, UAE University, Al Ain, UAE.

During the late afternoon and at night time, as the ambient temperature started decreasing, the relative humidity started increasing. The most ideal time to run the atmospheric water generation system or the time when the maximum amount of water can be generated is when the ambient air temperature is close to the dew point temperature (less than 10°C) at a higher relative humidity being around 1 AM at night. For the 2nd day of the experiment, the relative humidity remained above 40% for almost 17.5 hours from 1:00 PM to 5:30 AM. The difference between the dew point temperature and the ambient air temperature remained near 10°C for 13 hours, between 3:30 PM to 4:30 AM as shown in Figure 41. This is the more suitable time to run the AWG system to generate maximum water with low energy consumption. Almost the same trend was observed for the 3rd day of the experiment as the relative humidity remained above 40% for almost 15 hours from 2:00 PM to 5:00 AM. The difference between the dew point temperature and the ambient air temperature reduced below 10°C 5 PM to 4:00 AM. This difference reached up to a minimum of 2.3°C at 12:00 AM, as shown in Figure 42.

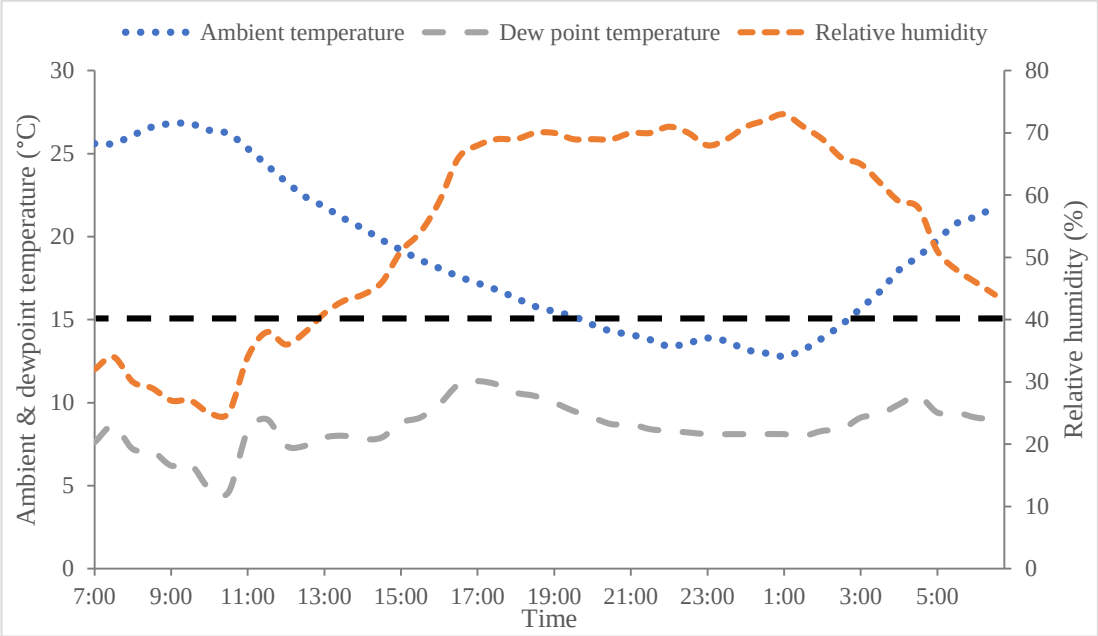

Figure 41: The measured humidity, ambient temperature and dewpoint and for the 2nd day of the experiment at the site in Falaj Hazza Campus, UAE University, Al Ain, UAE.

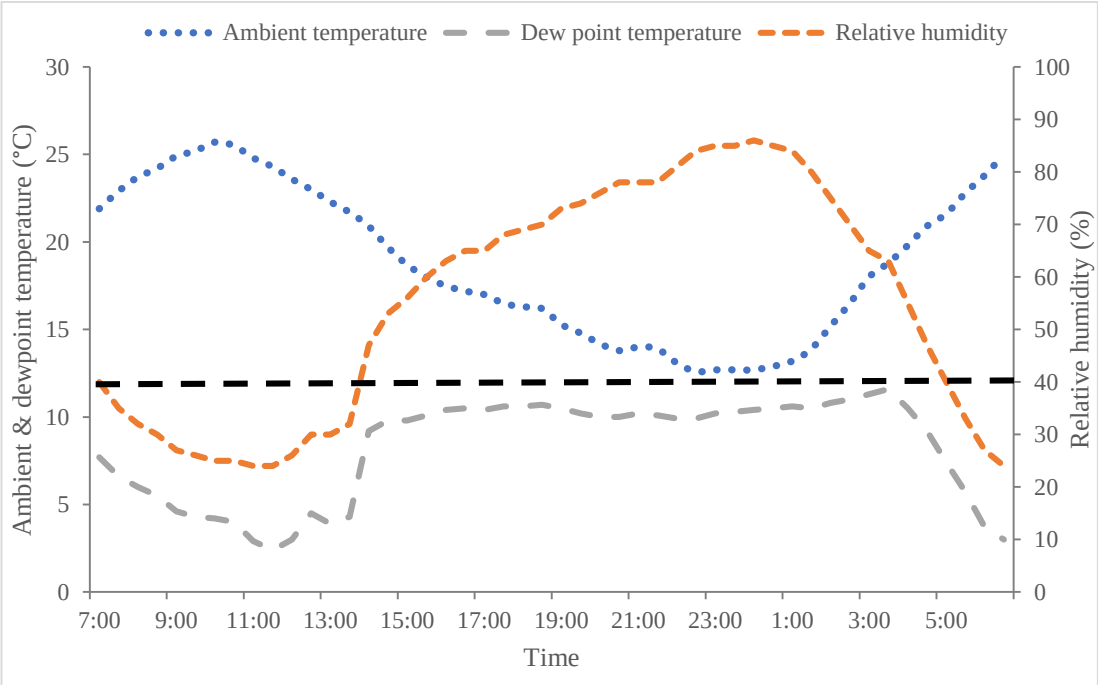

Figure 42: The measured humidity, temperature, dewpoint and Wind speed data for the 3rd day of the experiment at the site in Falaj Hazza Campus, UAE University, Al Ain, UAE.

5.5.2 Experimental results for AWG system

Many trials were conducted to check water production by using the AWG system. Ambient temperature, relative humidity and dew point temperature were also measured as elaborated in graphically and theoretically in the above section. The AWG system was run for 3 particular hours based on weather data in specific days to check the amount of atmospheric water generation. Usually, for this time interval, the humidity remained above 70% for the days of the experiment. A graph of water produced is plotted against the average and peak humidity of the air as shown in Figure 43. The average and peak relative humidity for that particular interval of time was above 70%.

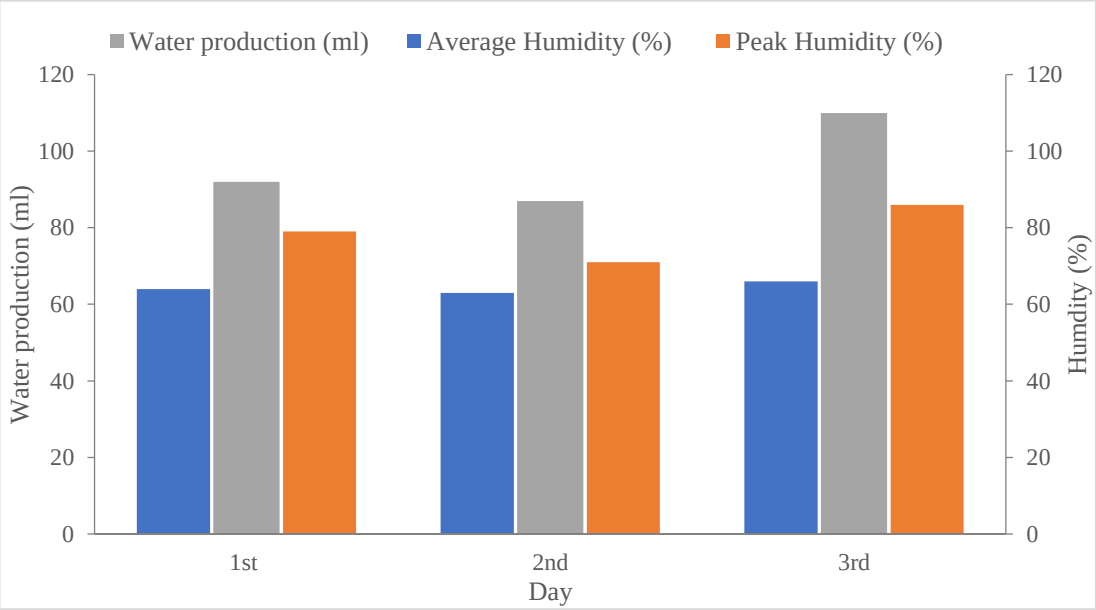

Figure 43: The produced water with respect to the average and peak humidity for the 1st, 2nd and 3rd day of the experiment at the site in Falaj Hazza Campus, UAE University, Al Ain, UAE.

The maximum water of 110 ml was produced on the 3rd day when the humidity reached up to 86% for that particular day and remained above 70% for almost 7 hours. The water production for the 1st and 2nd day was 92 ml and 87 ml respectively as shown in Figure 43. The rate of water production depends on the ambient temperature, humidity, the volume of air passing over the cooling plate, and the capacity of the device to cool the air. This reduces the air temperature, which in turn reduces the air's water vapour carrying capability. AWG system becomes more efficient with the rise in relative humidity and air temperature as it can be seen in Figure 44. For the 3rd day of the experiment, the ambient temperature increased as compared to the 1st day, but the more water generated on the 3rd day, because of the increase in humidity along with air temperature.

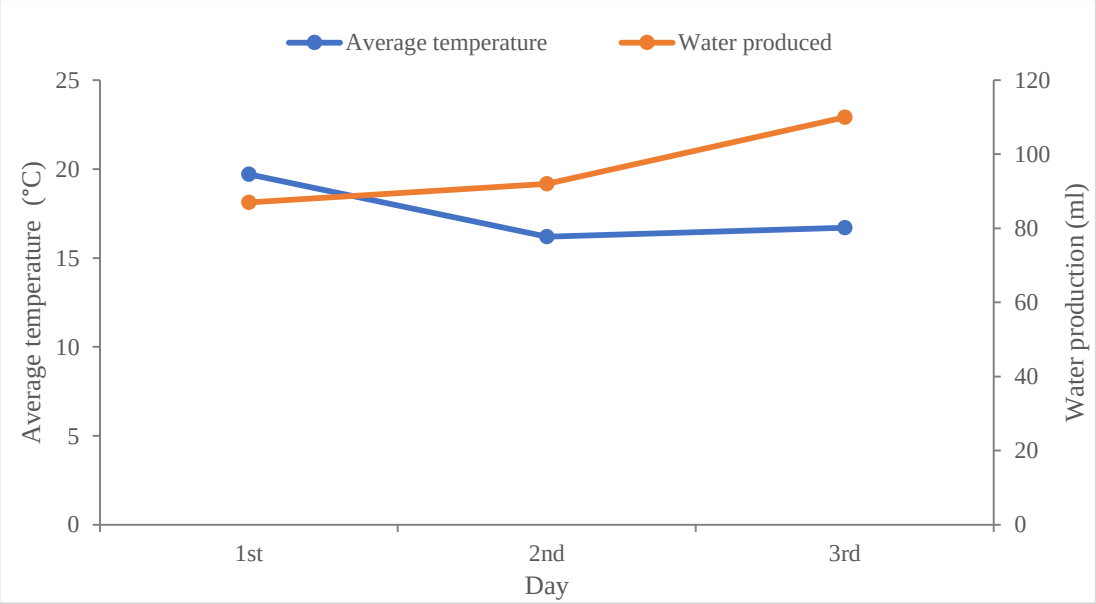

Figure 44: The produced water with respect to the ambient temperature for the 1st, 2nd and 3rd day of the experiment at the site in Falaj Hazza Campus, UAE University, Al Ain, UAE.

Novel water sprinkling techniques consume approximately 1 – 2 litre of water to clean 2 m^2 PV module. Extend this to plant scale a 1 MW of solar plant uses almost 7000 - 10000 litres of water in a single cycle to get clean. Usually, plant need to clean twice in a month, means 20,000 litres of water required to clean 1 MW solar plant in a month, which increases as the installed capacity. According to the measured values of power drop and water generation, the proposed cleaning frequency is 15 days. By using the developed AWG system, approximately 2 litres of water can be generated in 15 days in the specified conditions. This AWG system not only decreases the power drop and improves the efficiency of the plant, but it also saves the substantial amount of water (which can be used for domestic or irrigation purpose) by extracting water from the air.

5.6 Algorithmic approach for AWG system

To make the system fully automated, all the sensors (voltage sensor, current sensor, temperature sensor, dewpoint temperature sensor and humidity sensor) can be integrated into a control system. These sensors measure the atmospheric parameters that help decide to turn ON/OFF the AWGS through an algorithm. Referring to Figure 45, which is a schematic diagram showing the power generation, storage, power conversion and its utilization to generate atmospheric water. It comprises of photovoltaic and water generation system. When the solar radiations strike at the surface of the photovoltaic panel, PV panel produced the DC power that goes to the charge controller through the DC wires. The charge controller is a DC to Dc converter that draws the maximum voltage & current coming from the PV array and optimize them according to the battery/utility grid requirement. Then this regularized power from charge controller goes to the battery storage or utility grid through the DC wire

and that stored DC power can be used to run the atmospheric water generation system later on. Otherwise, solar power goes to the power inverter. Solar inverters are the devices that convert the DC power from PV panels into AC power then supplied to the AC loads. The DC power from PV cannot be directly transmitted to solar inverter because the power supplied to the inverter will not be tuned/regularized according to the inverter requirements.

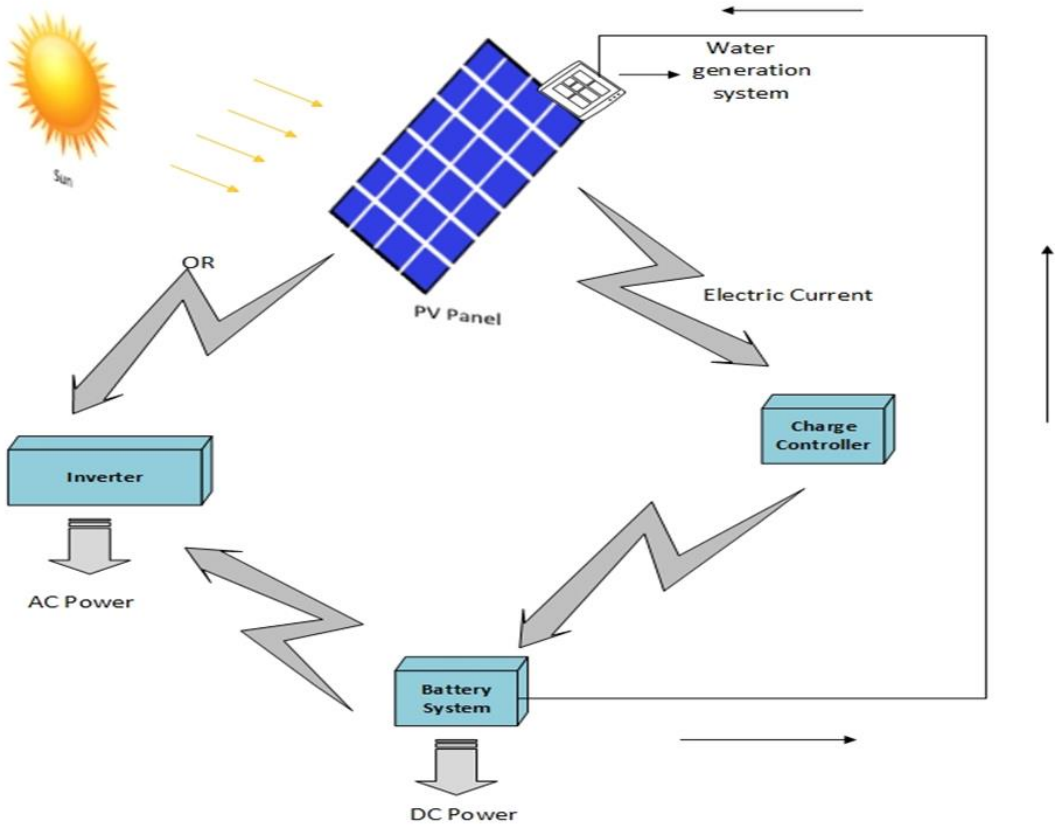

Figure 45: A general installation of PV atmospheric water generation system without the controller.

As can be seen from the complete AWGS setup Figure 46, PV panel placed under the solar radiations, which generates the electric power DC that goes directly to the controller. The controller comprises of different sensors, such as voltage sensor S1, current sensor S2, temperature sensor S3, dew point temperature sensor S4 and humidity sensor S5. The sensors calculate these parameters and help to direct DC power to inverter or battery based on the given conditions to the system. The algorithm E1 calculates the voltage and current and if their values are less than the minimum requirement to turn on the inverter, then it diverts the power towards the battery storage, otherwise, this will let it go towards the inverter. When the power from PV is greater than the minimum requirement of the inverter then the inverter operates and starts to converter the DC power to AC. When this AC power is connected to the grid**,** the grid has its own limitations of power input same as an inverter.

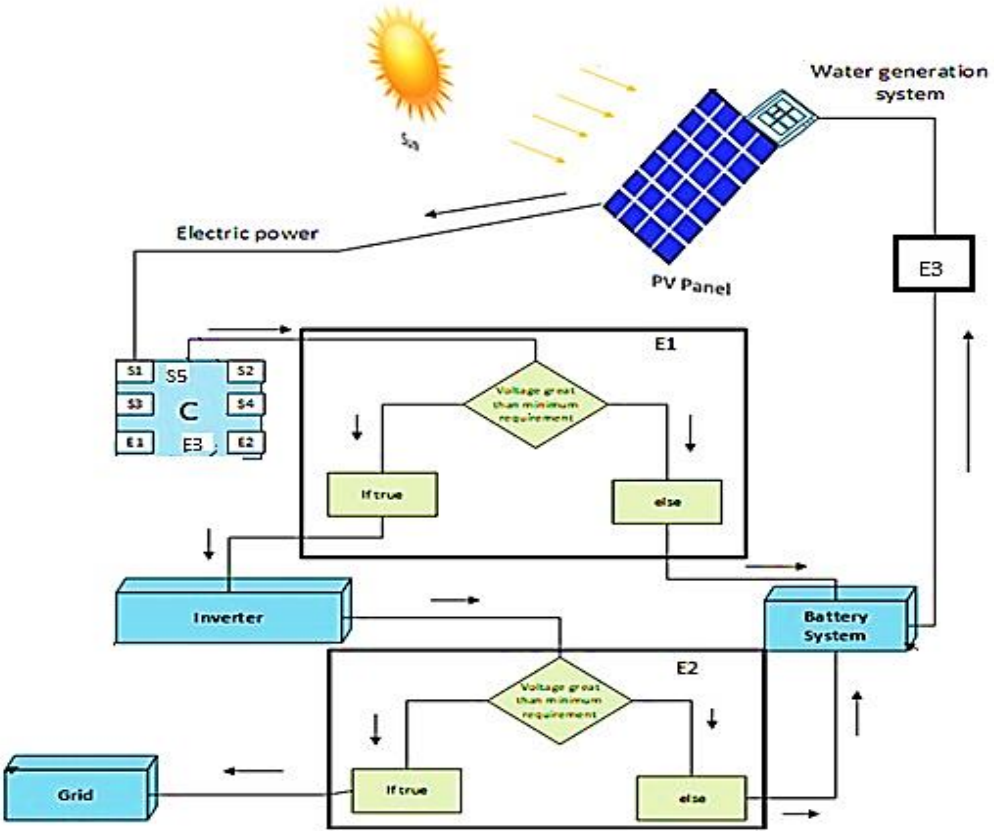

Figure 46: A complete setup of a system to provide atmospheric water using the wasted power produced by PV.

If the difference between the values of ambient temperature sensor and the dew point temperature sensors is less than 10°C or any preset value (because when the ambient air temperature is close to the dew point temperature at that time, very small amount of energy and time required to drop the air temperature at the dew point temperature level, where the vapours condense to generate water droplets) and the measured value by humidity sensors is greater than 70% (or any predefined value) then the algorithm E3 will turn on the AWG system automatically by taking power from battery storage. The AWGS will operate only at the specified time and conditions (humidity & temperature) set by the user.

5.7 Simulink model development for PV-AWG system

A simplest equivalent circuit of a solar cell is a current source in parallel with a diode. The output of the current source is directly proportional to solar energy (photons) that hits on the solar cell (photocurrent Iph). During darkness, the solar cell is not an active device; it works as a diode, i.e. a p-n junction. It produces neither a current nor a voltage. However, if it is allowed to connect to an external source (large voltage) it generates a current Id, called diode (D) current or dark current. The diode determines the IV characteristics of the cell. A simple circuit diagram of the solar cell is shown in Figure 47, which includes a photo-current, diode, parallel and series resistor [102].

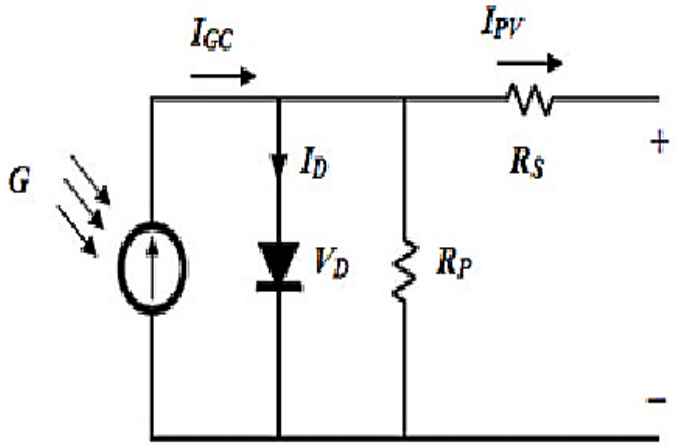

Figure 47: Simple circuit diagram of solar cell

Model for the PV developed by using the below-mentioned Eq. 7-13 [103, 104] and the PV specifications that are already explained in Chapter 3.

$$V_t = \frac{KT_{op}}{q} \quad \text{(Eq. 7)}$$

$$V_{oc} = V_t \ln\left(\frac{I_{ph}}{I_s}\right) \quad \text{(Eq. 8)}$$

$$I_d = \left[e^{\frac{(V+IR_S)}{(nV_tCN_S)-1}}\right] I_s N_p \quad \text{(Eq. 9)}$$

$$I_s = I_{rs}\left(\frac{T_{op}}{T_{ref}}\right)^3 e^{\left[\frac{qE_g}{nk}\left(\frac{1}{Top}-\frac{1}{Tref}\right)\right]} \quad \text{(Eq. 10)}$$

$$I_{rs} = \frac{I_{sc}}{\left[e^{\left(\frac{V_{OC}q}{KCT_{op}n}\right)}-1\right]} \quad \text{(Eq. 11)}$$

$$I_{sh} = \frac{V+IR_S}{R_p} \quad \text{(Eq. 12)}$$

$$I = I_{ph}N_p - I_d - I_{sh} \quad \text{(Eq. 13)}$$

The proposed model was simulated using MATLAB Simulink. The system consists of a PV panel, battery bank, controller, inverter and converters. The Simulink model of the PV circuit to check for I-V and P-V characteristics curves are shown in Figure 48.

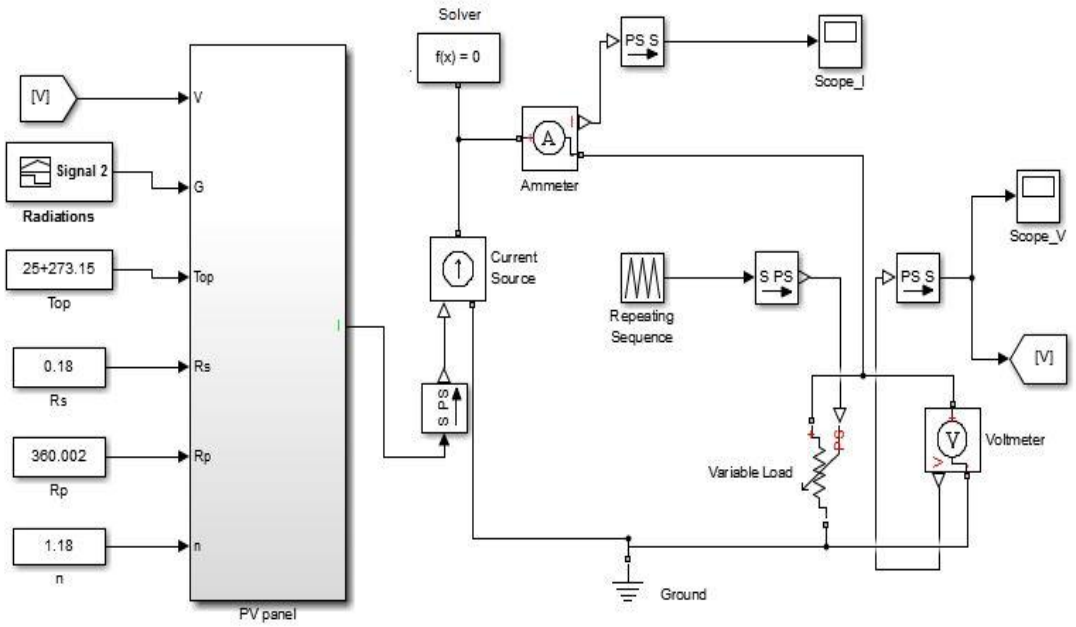

Figure 48: Simulink model of the PV circuit to check for I-V and P-V characteristics curves.

Further, the Simulink model was enhanced by integrating the DC-DC converter, battery system, boost converter, DC-AC inverter, 78 W load (AWG system) and the algorithm to run the AWG system based on the values provided by the different sensors. Batteries get damaged and their life diminishes by directly charging through solar PV modules due to the unregulated voltage and current supplied by them. Solar DC-DC converter (buck converter) regulates the charging current/voltage supplied by the PV modules according to the battery specifications/requirements. These problems led to high demand for efficient DC-DC converters [105]. A simple buck converter schematic is shown in Figure 49 [106].

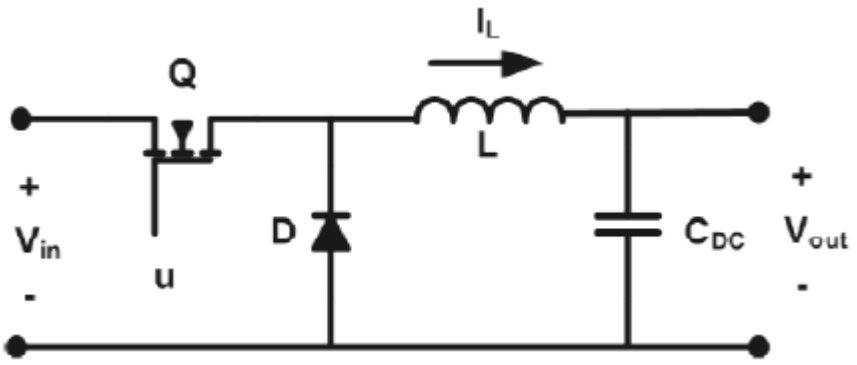

Figure 49: Circuit diagram of the buck converter.

Furthermore, there are fluctuations in the output DC voltages generated by PV modules due to the uneven/uncontrolled soar radiations, dust adhering at the surface, ambient temperature variations and the shadowing effects [107, 108]. Therefore, a DC-DC boost converter is crucial in order to control the low and incoherent DC voltage output from PV modules. It's not just only step up or down the DC output voltages generated by the PV modules but also perform a key task by extracting maximum power at different conditions during the day on the basis of I-V characteristics of PV modules by using the algorithm of maximum power point tracking (MPPT) [109]. A complete model diagram is shown below in Figure 50. After the boost coverter, the voltage goes into DC-AC inverter which converts the voltages from DC to AC. The Simulink design to turn ON/OFF the 78 W AWG system as per the algorithm (as explained above) shown in Figure 51. It allows AWGS to take power from storage after fulfilling the requirements of the pre-defined algorithm.

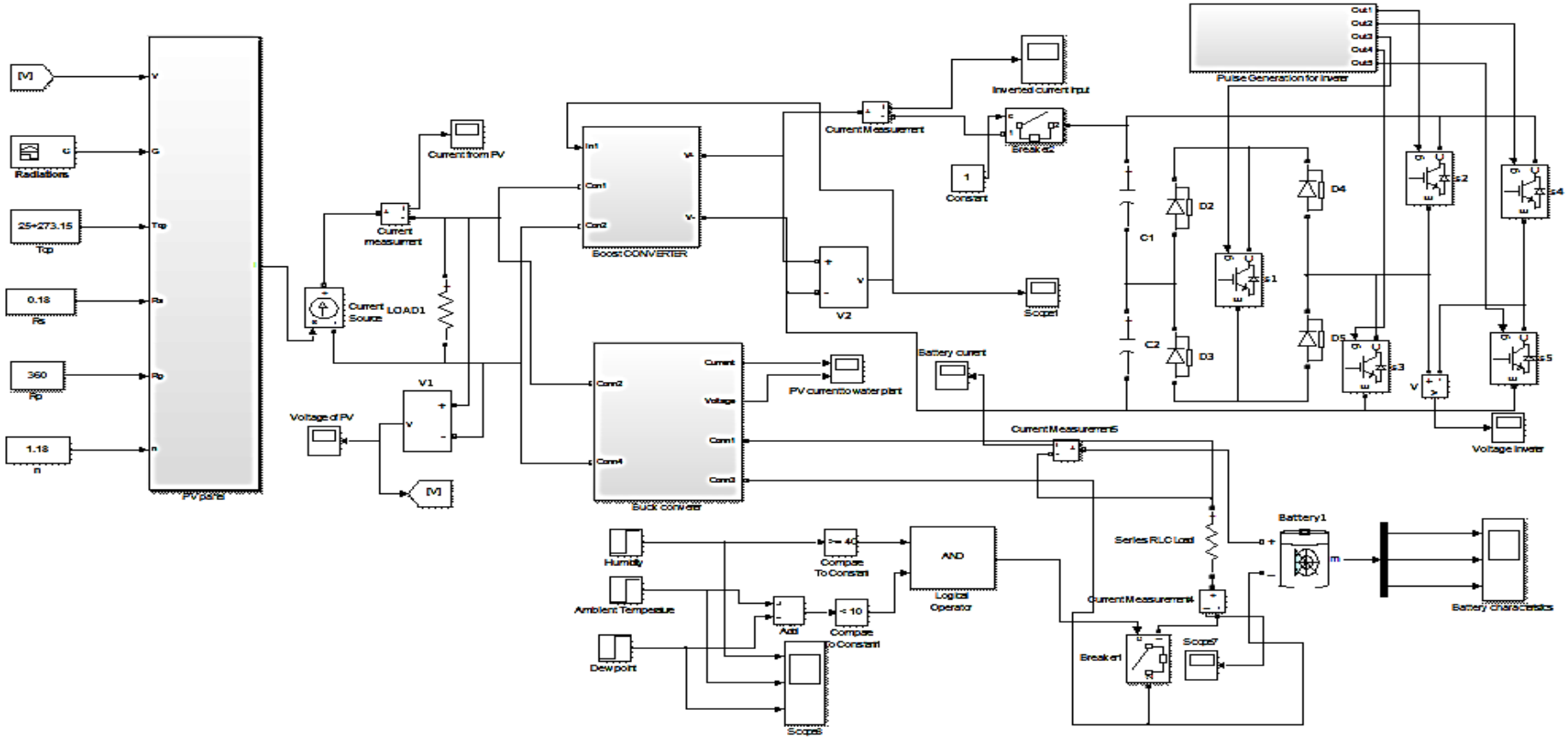

Figure 50: A complete Simulink model diagram for PV AWG system.

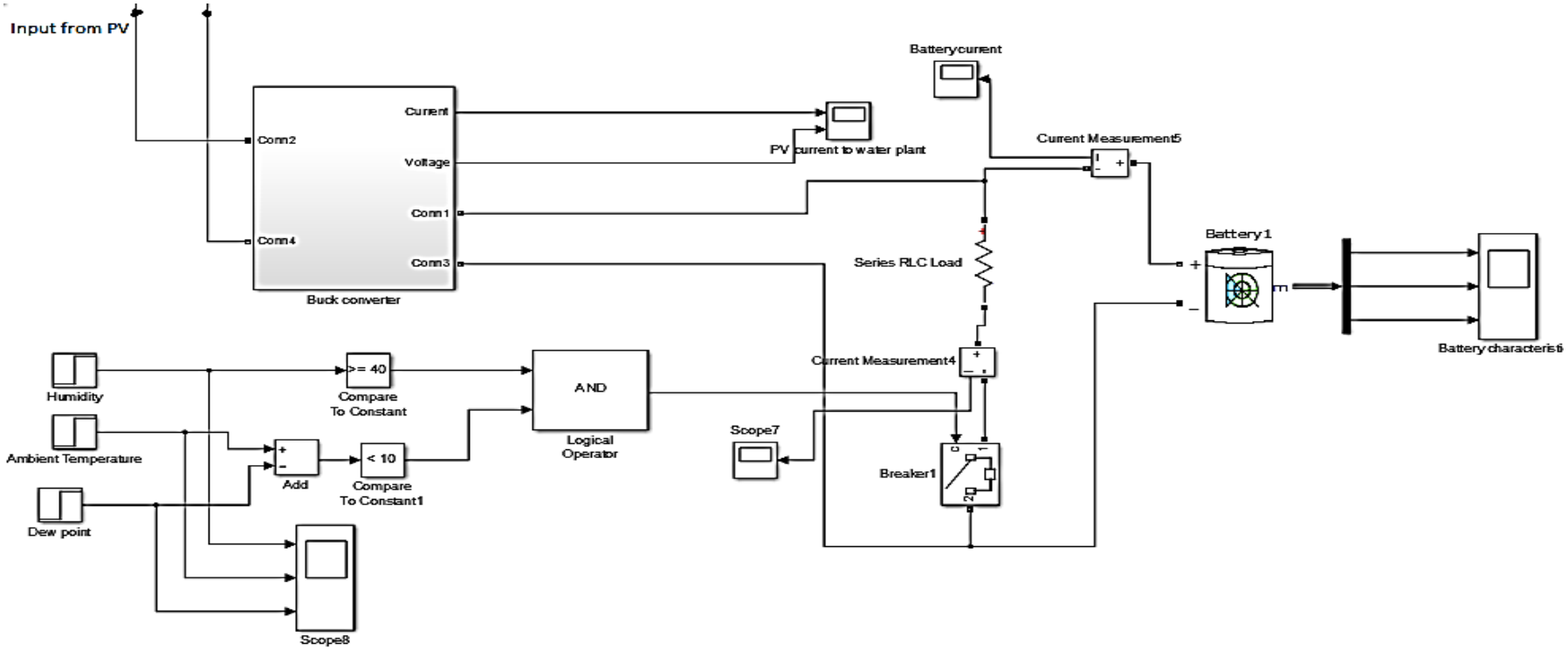

Figure 51: Simulink model for AWG system with battery connected.

5.8 Simulation result

Photovoltaic I-V curve provides a detailed description of the energy conversion ability and efficiency of the PV module or cell with current and voltage (I-V) characteristics. Figure 52 shows the I-V characteristics of a solar panel that works under 25°C operating temperature. With the open-circuit solar cell connected to no load, the current is at its lowest point, and the voltage is maximum across the cell, known as the open-circuit voltage (V_{OC}) of a solar cell. On the other end, when the solar cell is short-circuited by connecting the positive and negative leads the voltage over the cell is at its lowest level but the current flowing out of the cell is at maximal, called the short circuit current (I_{SC}) [110].

The power supplied by a PV panel comes from the product of each point (voltage and current) in the I-V curve. The maximum power point (MPP) is a point at P-V characteristics curve where the product of I-V yields the highest value thus enabling the solar module to deliver maximum electrical power [111]. I-V and P-V curves of solar modules enable to achieve their characteristic parameters, such as Isc, Voc, MPP and FF deemed crucial to design the PV system. The I-V and P-V curves rely on the operating temperature, solar radiations and their spectral distribution [108]. Table 10 shows the calculated module data at standard test conditions (STC) Top = 25ºC and air mass (AM) = 1.5.

Table 10: PV measured parameters through simulation.

Parameters	**Values**
Vmpp	35.73
Impp	4.589
Pmpp	163.89

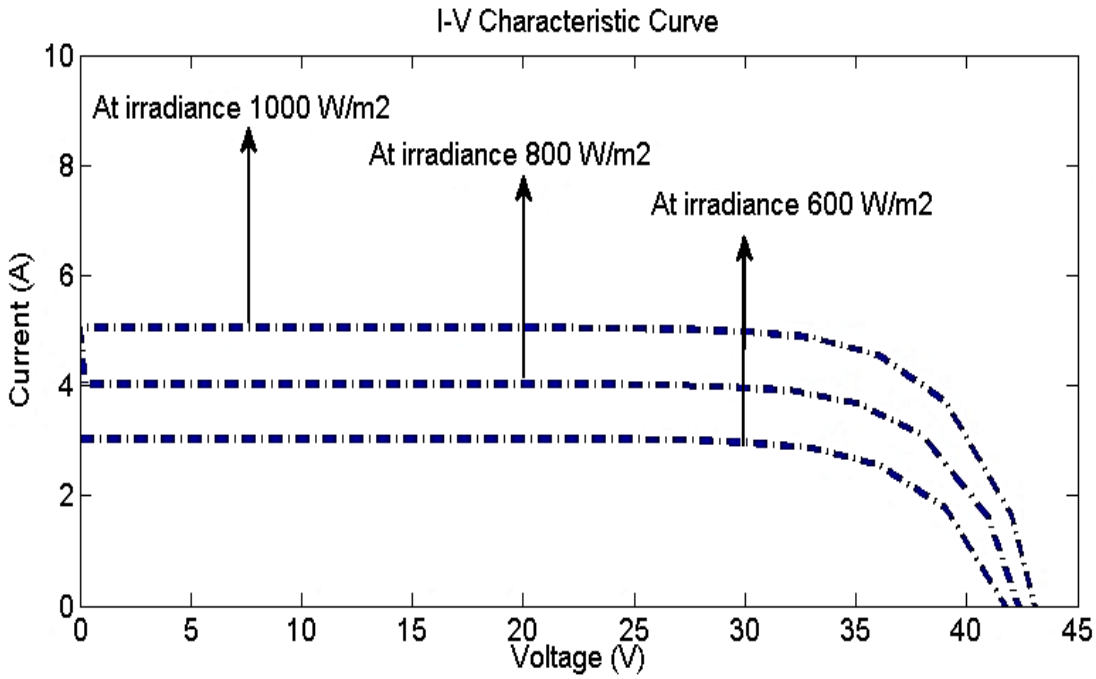

Figure 52: I-V curves at different radiations, 1000, 800 and 600 W/m2 with Top= 25C and AM=1.5.

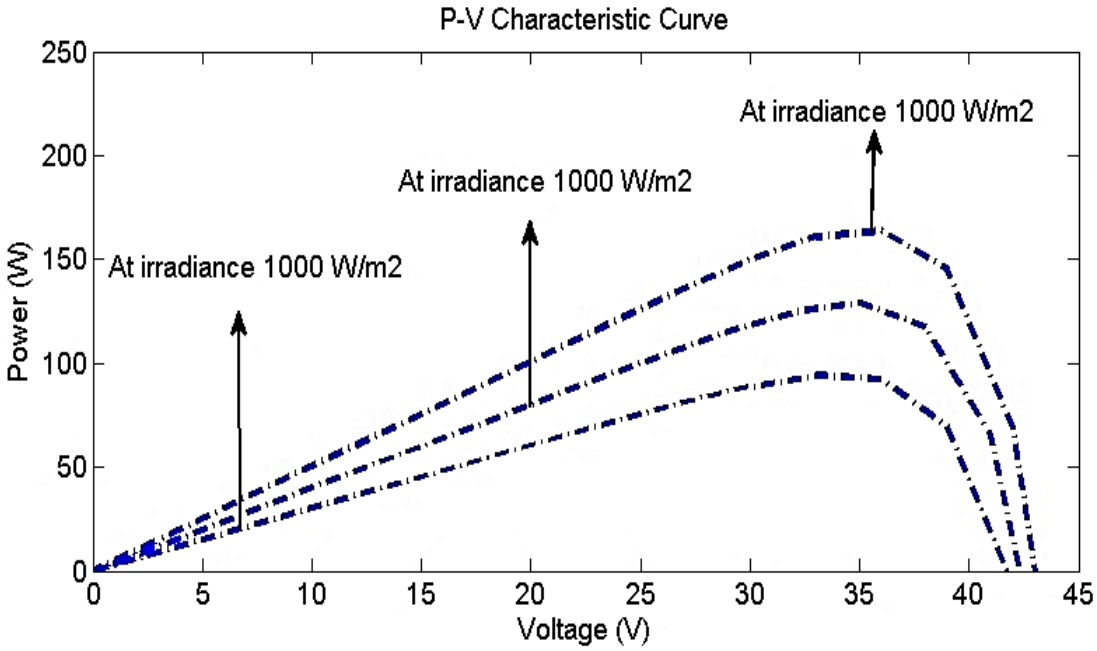

Figure 53: P-V curves at different radiations, 1000, 800 and 600 W/m2 with Top= 25C and AM=1.5.

As it can be seen from the both I-V and P-V curves in the above Figures 52 and 53 that there is a nominal drop in V_{OC} but a significant reduction in I_{SC} by changing the radiation level with the same operating temperature and the other parameters.

The scop output of battery characteristics in Figure 55, which shows that the battery started to discharge by supplying the power to AWG load between the time interval of 0.07 - 0.1 when the difference between the values of ambient temperature and the dew point temperature re aches less than 10°C and the humidity value is greater than 40 as shown in Figure 54.

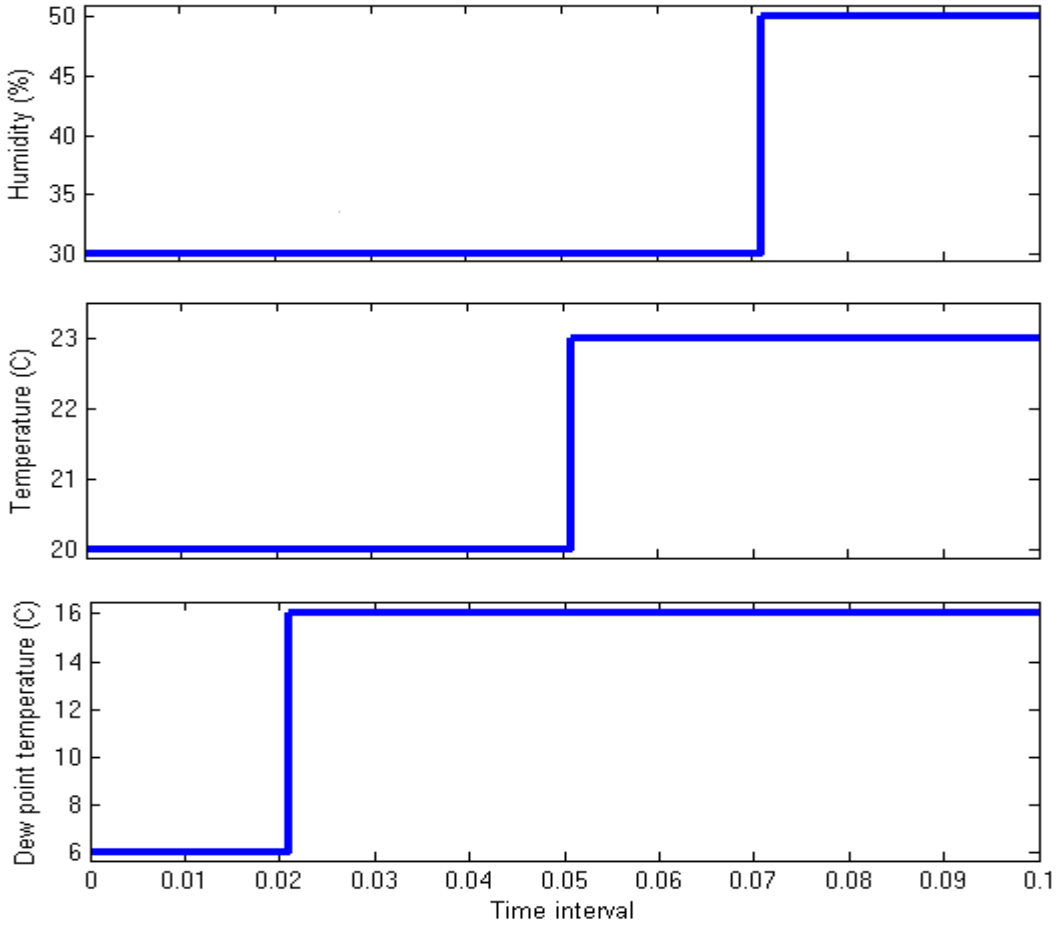

Figure 54: Humidity, ambient temperature and dew point temperature sensors values between time interval 0 - 0.1.

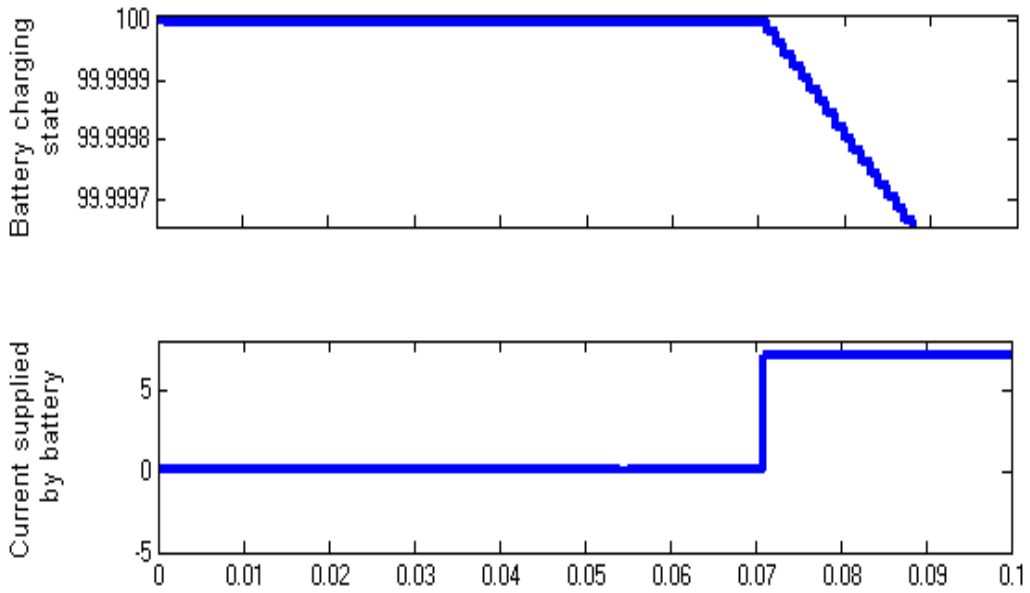

Figure 55: Battery characteristics between 0 - 0.1 time interval.

The initial investigations were done at one location for the atmospheric water generation that will extend to further locations with different ambient conditions (i.e. ambient temperature, humidity, dew point temperature, wind speed etc.) in future. Future research will also focus on the detailed plant scale research and development of modelling algorithms to validate the experiment.

Chapter 6: Conclusion

In the present research, the cleaning frequency of solar panels from accumulated dust through experimentation in UAE conditions was measured that helped to design the “Self-water-generation system” for cleaning solar panels.

To measure the pure radiations losses caused by the dust, five transparent glasses with 3 mm thickness used in this research. Pyranometers were installed at the back sides of transparent glasses, and one is installed at the latitude angle at the upper side of glass modules to measure solar radiation intensity falling on each module's surface before and after the transmitting through the glass. One of the reference glass modules has been cleaned on a daily basis, while the other four has been cleaned after 10 days, 20 days, 30 days and seasonal basis respectively.

The average and peak radiation penetration difference of 43 W/m^2 and 87 W/m^2 respectively were observed between a daily clean glass module and for the module kept dusted for 10 days. The average and peak radiation transmission difference through the glass module reach up to 57 W/m^2 and 118 W/m^2 respectively for the daily clean glass module and the module cleaned after 20 days. It was noted that the peak and average radiation penetration to PV module dropped by 120 W/m^2 65 W/m^2 respectively for the daily cleaned and monthly cleaned PV panels. The drop in radiation substantially increased to a peak value of 239 W/m^2 and an average value of 119 W/m^2 for a module cleaned after 3 months compared to a daily cleaned module.

The power losses caused by dust are also calculated and compared the powers produced by the clean and the dusty PV panels. In the UAE atmospheric conditions with no major sandstorm, if PV don’t get cleaned for 10 days, it causes the 3% drop in electric power. The PV produced 5% less power when does not get cleaned for 20

days as compared to the daily cleaned PV panel. Power loss reached to 7% for a dusted panel for one month and 13% for a dusted panel for three months.

Three days of trials were conducted to assess the water production by using the AWG system to clean the PV from the PV power. The AWG system was run for 3 hours per night for particular days to determine the amount of water generation. The maximum water production of 110 ml per night (3 hours) was achieved in the best case during the experiments when the humidity remained above 70% and peaked at 86%. The water production remained close enough for the rest of two days being 92 ml and 87 ml. According to the measured values of power drop and water generation, the proposed cleaning frequency is 15 days.

A Simulink model for a module developed and the I-V and P-V characteristics of used panel measured and verified through simulation results. Algorithm to turn ON/OFF the AWG system on the basis of weather data was also developed and tested by running the simulation model.

References

[1] M. Hasanuzzaman, U. Zubir, N. Ilham and H. Seng Che, "Global electricity demand, generation, grid system, and renewable energy policies: a review", Wiley Interdisciplinary Reviews: Energy and Environment, vol. 6, no. 3, p. e222, 2016. Available: 10.1002/wene.222

[2] "World Energy Consumption Statistics | Enerdata", Yearbook.enerdata.net, 2019. Available: https://yearbook.enerdata.net/total-energy/world-consumption-statistics.html. [Accessed: 02 Nov 2018].

[3] N. Abas, A. Kalair and N. Khan, "Review of fossil fuels and future energy technologies", Futures, vol. 69, pp. 31-49, 2015. Available: 10.1016/j.futures.2015.03.003.

[4] M. Riffat SB, "Building Energy Consumption and Carbon dioxide Emissions: Threat to Climate Change", Journal of Earth Science & Climatic Change, vol. 3, 2015. Available: 10.4172/2157-7617.s3-001.

[5] "Renewables 2018: Key Findings", Iea.org, 2018. Available: https://www.iea.org/renewables2018/. [Accessed: 13 Nov 2018].

[6] G. Kavlak, J. McNerney and J. Trancik, "Evaluating the causes of cost reduction in photovoltaic modules", Energy Policy, vol. 123, pp. 700-710, 2018. Available: 10.1016/j.enpol.2018.08.015.

[7] "TCEP: Solar PV", Iea.org, 2019. Available: https://www.iea.org/tcep/power/renewables/solarpv/. [Accessed: 13 Dec 2018].

[8] "Clean Energy Investment 2018 | Bloomberg NEF", BloombergNEF, 2019. Available: https://about.bnef.com/clean-energy-investment/. [Accessed: 13 Dec 2018].

[9] H. Gunerhan, A. Hepbasli and U. Giresunlu, "Environmental Impacts from the Solar Energy Systems", Energy Sources, Part A: Recovery, Utilization, and Environmental Effects, vol. 31, no. 2, pp. 131-138, 2008. Available: 10.1080/15567030701512733.

[10] S. Grover, "Energy, Economic, and Environmental Benefits of the Solar America Initiative", National Renewable Energy Laboratory (NREL), 2007.

[11] P. Owusu and S. Asumadu-Sarkodie, "A review of renewable energy sources, sustainability issues and climate change mitigation", Cogent Engineering, vol. 3, no. 1, 2016. Available: 10.1080/23311916.2016.1167990.

[12] M. Shaikh, "A Review Paper on Electricity Generation from Solar Energy", International Journal for Research in Applied Science and Engineering Technology, vol., no., pp. 1884-1889, 2017. Available: 10.22214/ijraset.2017.9272.

[13] R. Lambert and P. Silva, "The challenges of determining the employment effects of renewable energy", Renewable and Sustainable Energy Reviews, vol. 16, no. 7, pp. 4667-4674, 2012. Available: 10.1016/j.rser.2012.03.072.

[14] B. Johansson, "Security aspects of future renewable energy systems–A short overview", Energy, vol. 61, pp. 598-605, 2013. Available: 10.1016/j.energy.2013.09.023.

[15] IRENA, "Renewable Power Generation Costs in 2017", IRENA, Abu Dhabi, 2018.

[16] "World Energy Statistics | Enerdata", Enerdata, 2018. Available: https://yearbook.enerdata.net/. [Accessed: 14 Dec 2018].

[17] "Basic research needs for solar energy utilization", Argonne National Laboratory, United States, 2005.

[18] A. Husain, W. Hasan, S. Shafie, M. Hamidon and S. Pandey, "A review of transparent solar photovoltaic technologies", Renewable and Sustainable Energy Reviews, vol. 94, pp. 779-791, 2018. Available: 10.1016/j.rser.2018.06.031.

[19] J. Zhang, M. Shin, Z. Dai, L. Zhang, X. He, W. Cheng, M. Cao and G. Zou, "Enlarging photovoltaic effect: combination of classic photoelectric and ferroelectric photovoltaic effects", Scientific Reports, vol. 3, no. 1, 2013. Available: 10.1038/srep02109.

[20] D. Chapin, C. Fuller and G. Pearson, "A New Silicon p-n Junction Photocell for Converting Solar Radiation into Electrical Power", Journal of Applied Physics, vol. 25, no. 5, pp. 676-677, 1954. Available: 10.1063/1.1721711.

[21] A. Makki, S. Omer and H. Sabir, "Advancements in hybrid photovoltaic systems for enhanced solar cells performance", Renewable and Sustainable Energy Reviews, vol. 41, pp. 658-684, 2015. Available: 10.1016/j.rser.2014.08.069.

[22] A. Mohiuddin, M. Bin Sabarudin, A. Ali Khan and S. Ihsan, "Design and development of hybrid energy generator (photovoltaics) with solar tracker", IOP Conference Series: Materials Science and Engineering, vol. 184, p. 012043, 2017. Available: 10.1088/1757-899x/184/1/012043.

[23] "Solar Power Energy with its Advantages and Disadvantages", ElProCus, 2019. Available: https://www.elprocus.com/solar-power-energy-with-advantages-and-disadvantages. [Accessed: 20 Dec 2018].

[24] X. Wang, H. Lu, H. Ni, W. Lu, M. Zhang and Y. Zhang, "Research Progress of Border for Solar Photovoltaic Modules", Proceedings of the International Conference on Chemical, Material and Food Engineering, 2015. Available: 10.2991/cmfe-15.2015.69

[25] "Module Materials", Pveducation.org, 2019. Available: https://www.pveducation.org/pvcdrom/modules/module-materials. [Accessed: 27 Jan 2019].

[26] A. El Amrani, A. Mahrane, F. Moussa and Y. Boukennous, "Solar Module Fabrication", International Journal of Photoenergy, vol. 2007, pp. 1-5, 2007. Available: 10.1155/2007/27610.

[27] M. Kempe, "Encapsulant Materials for PV Modules", in Photovoltaic Solar Energy: From Fundamentals to Applications, John Wiley & Sons, 2019, pp. 478-490.

[28] A. Hasan, J. Sarwar and A. Shah, "Concentrated photovoltaic: A review of thermal aspects, challenges and opportunities", Renewable and Sustainable Energy Reviews, vol. 94, pp. 835-852, 2018. Available: 10.1016/j.rser.2018.06.014.

[29] K. Geretschläger, G. Wallner and J. Fischer, "Structure and basic properties of photovoltaic module back sheet films", Solar Energy Materials and Solar Cells, vol. 144, pp. 451-456, 2016. Available: 10.1016/j.solmat.2015.09.060.

[30] G. Illya, V. Handara, M. Siahandan, A. Nathania and A. Budiman, "Mechanical Studies of Solar Photovoltaics (PV) Backsheets Under Salt Damp Heat Environments", Procedia Engineering, vol. 215, pp. 238-245, 2017. Available: 10.1016/j.proeng.2017.12.144.

[31] J. Kalejs, "Junction box wiring and connector durability issues in photovoltaic modules," in Proceedings of SPIE - The International Society for Optical Engineering, 2014, Available: 10.1117/12.2063488.

[32] M. Lokesh, P. Kumara, S. Aneel, T. Sudhakar and N. Rajasekar, “Comparative study on charge controller techniques for solar PV system” Energy Procedia, vol. 117, pp. 1070–1077, 2017.

[33] S. Salman, X. AI and Z. WU, "Design of a P-&-O algorithm based MPPT charge controller for a stand-alone 200W PV system", Protection and Control of Modern Power Systems, vol. 3, no. 1, pp. 1-8, 2018. Available: 10.1186/s41601-018-0099-8.

[34] E. Radziemska, "The effect of temperature on the power drop in crystalline silicon solar cells", Renewable Energy, vol. 28, no. 1, pp. 1-12, 2003. Available: 10.1016/s0960-1481(02)00015-0.

[35] B. Mondoc, F. Romania, “Factor influencing the performance of Photovoltaic power plant” 3rd International Conference on Modern Power system, 2010, Available: https://ie.utcluj.ro/files/acta/2010/Number5/MPS_2010_Mondoc.pdf

[36] A. Ghitas, "Studying the effect of spectral variations intensity of the incident solar radiation on the Si solar cells performance", NRIAG Journal of Astronomy and Geophysics, vol. 1, no. 2, pp. 165-171, 2012. Available: 10.1016/j.nrjag.2012.12.013.

[37] W. Okullo, M. Munji, F. Vorster and E. van Dyk, "Effects of spectral variation on the device performance of copper indium diselenide and multi-crystalline silicon photovoltaic modules", Solar Energy Materials and Solar Cells, vol. 95, no. 2, pp. 759-764, 2011. Available: 10.1016/j.solmat.2010.10.018.

[38] W. van Sark, A. Meijerink, R. Schropp, J. van Roosmalen and E. Lysen, "Enhancing solar cell efficiency by using spectral converters", Solar Energy Materials and Solar Cells, vol. 87, no. 1-4, pp. 395-409, 2005. Available: 10.1016/j.solmat.2004.07.055.

[39] J. Cano, J. John, S. Tatapudi and G. Tamizhmani, "Effect of tilt angle on soiling of photovoltaic modules", in 2014 IEEE 40th Photovoltaic Specialist Conference, PVSC 2014, Denver, United States, 2019.

[40] R. Santbergen and R. van Zolingen, "The absorption factor of crystalline silicon PV cells: A numerical and experimental study", Solar Energy Materials and Solar Cells, vol. 92, no. 4, pp. 432-444, 2008. Available: 10.1016/j.solmat.2007.10.005.

[41] H. Yang, H. Wang, D. Cao, D. Sun and X. Ju, "Analysis of Power Loss for Crystalline Silicon Solar Module during the Course of Encapsulation", International Journal of Photoenergy, vol. 2015, pp. 1-5, 2015. Available: 10.1155/2015/251615.

[42] Z. Lu and Q. Yao, "Energy analysis of silicon solar cell modules based on an optical model for arbitrary layers", Solar Energy, vol. 81, no. 5, pp. 636-647, 2007. Available: 10.1016/j.solener.2006.08.014.

[43] J. Yoo, J. Cho, K. Han and J. Yi, "RIE surface texturing for optimum light trapping in multicrystalline silicon solar cells", Journal of the Korean Physical Society, vol. 60, no. 12, pp. 2071-2074, 2012. Available: 10.3938/jkps.60.2071.

[44] E. Baquedano, L. Torné, P. Caño and P. Postigo, "Increased Efficiency of Solar Cells Protected by Hydrophobic and Hydrophilic Anti-Reflecting Nanostructured Glasses", Nanomaterials, vol. 7, no. 12, p. 437, 2017. Available: 10.3390/nano7120437.

[45] "PV research cell record efficiency chart", Nrel.gov, 2019. Available: https://www.nrel.gov/pv/assets/pdfs/pv-efficiency-chart.20190103.pdf. [Accessed: 30 Jan 2019].

[46] B. Jiang, J. Ji and H. Yi, "The influence of PV coverage ratio on thermal and electrical performance of photovoltaic-Trombe wall", Renewable Energy, vol. 33, no. 11, pp. 2491-2498, 2008. Available: 10.1016/j.renene.2008.02.001.

[47] K. Emery, "Temperature dependence of photovoltaic cells," in Conference Record of the Twenty Fifth IEEE Photovoltaic Specialists Conference - 1996, Washington DC, 1996.

[48] J. Sarwar, S. McCormack, M. Huang, B. Norton, "Numerical validation of experimental temperature evolution in photovoltaic cells with varying ambient conditions," UK-ISES, pp. 1-4, 2011.

[49] M. Chaaban, "Temperature and PV performance optimization," Available: https://www.e-education.psu.edu/ae868/node/878. [Accessed: 30 Jan 2019].

[50] A. Mondal and K. Bansal, "A brief history and future aspects in automatic cleaning systems for solar photovoltaic panels", Advanced Robotics, vol. 29, no. 8, pp. 515-524, 2015. Available: 10.1080/01691864.2014.996602.

[51] O. Bubnova, "Photovoltaics: Self-cleaning solar cells", Nature Nanotechnology, 2016. Available: 10.1038/nnano.2015.327.

[52] W. Tian, Y. Wang, J. Ren and L. Zhu, "Effect of urban climate on building integrated photovoltaics performance", Energy Conversion and Management, vol. 48, no. 1, pp. 1-8, 2007. Available: 10.1016/j.enconman.2006.05.015.

[53] M. El-Shobokshy and F. Hussein, "Degradation of photovoltaic cell performance due to dust deposition on to its surface", Renewable Energy, vol. 3, no. 6-7, pp. 585-590, 1993. Available: 10.1016/0960-1481(93)90064-n.

[54] G. He, C. Zhou and Z. Li, "Review of Self-Cleaning Method for Solar Cell Array", Procedia Engineering, vol. 16, pp. 640-645, 2011. Available: 10.1016/j.proeng.2011.08.1135.

[55] M. Abu-Naser, "Solar Panels Cleaning Frequency for Maximum Financial Profit", Open Journal of Energy Efficiency, vol. 06, no. 03, pp. 80-86, 2017. Available: 10.4236/ojee.2017.63006.

[56] P. Denholm, E. Drury, R. Margolis and M. Mehos, "Solar Energy", Generating Electricity in a Carbon-Constrained World, pp. 271-302, 2010. Available: 10.1016/b978-1-85617-655-2.00010-9.

[57] Rollingwash, "Efficient and water-saving cleaning of the PV," Available: http://rollingwash.net/docs/Solar%20panels%20cleaning.pdf. [Accessed: 07 Feb 2019].

[58] M. Mani and R. Pillai, "Impact of dust on solar photovoltaic (PV) performance: Research status, challenges and recommendations", Renewable and Sustainable Energy Reviews, vol. 14, no. 9, pp. 3124-3131, 2010. Available: 10.1016/j.rser.2010.07.065.

[59] Z. Ahmed, H. Kazam and K. Sopian, "Effect of Dust on Photovoltaic Performance Review and Research Status" Latest Trends in Renewable Energy and Environmental Informatics, Malaysia, 2013.

[60] A. Hegazy, "Effect of dust accumulation on solar transmittance through glass covers of plate-type collectors", Renewable Energy, vol. 22, no. 4, pp. 525-540, 2001. Available: 10.1016/s0960-1481(00)00093-8.

[61] F. Mani, S. Pulipaka and R. Kumar, "Characterization of power losses of a soiled PV panel in Shekhawati region of India", Solar Energy, vol. 131, pp. 96-106, 2016. Available: 10.1016/j.solener.2016.02.033.

[62] J. Kaldellis and M. Kapsali, "Simulating the dust effect on the energy performance of photovoltaic generators based on experimental measurements", Energy, vol. 36, no. 8, pp. 5154-5161, 2011. Available: 10.1016/j.energy.2011.06.018.

[63] R. Gaier, M. Davis "Effect of particle size of Martian dust on the degradation of photovoltaic cell performance," NASA Technical Memorandum, Hawaii, 1992.

[64] J. Zhu, C. Hsu, Z. Yu, S. Fan and Y. Cui, "Nanodome Solar Cells with Efficient Light Management and Self-Cleaning", Nano Letters, vol. 10, no. 6, pp. 1979-1984, 2010. Available: 10.1021/nl9034237.

[65] G. Landis, "Mars Dust-Removal Technology", Journal of Propulsion and Power, vol. 14, no. 1, pp. 126-128, 1998. Available: 10.2514/2.5258.

[66] M. Al-Housani, Y. Bicer and M. Koç, "Assessment of Various Dry Photovoltaic Cleaning Techniques and Frequencies on the Power Output of CdTe-Type Modules in Dusty Environments", Sustainability, vol. 11, no. 10, p. 2850, 2019. Available: 10.3390/su11102850.

[67] M. Hudedmani, G. Joshi, R. Umayal and A. Revankar, "A Comparative Study of Dust Cleaning Methods for the Solar PV Panels", Advanced Journal of Graduate Research, vol. 1, no. 1, pp. 24-29, 2017. Available: 10.21467/ajgr.1.1.24-29.

[68] V. Saravanan, S. Darvekar, "Solar Photovoltaic Panels Cleaning Methods A Review", vol. 18, no. 24, pp. 1-17, 2018. ISSN: 1314-3395

[69] Q. Zhang, "A solar panel cleaning system based on a linear piezoelectric actuator" in IEEE, China, 2014.

[70] National Instruments, "cDAQ-9178 Compact DAQ Chassis," Available: http://www.ni.com/en-lb/support/model.cdaq-9178.html. [Accessed: 28- Feb - 2019].

[71] National Instruments, "C Series Temperature Input Module NI-9213," Available: http://www.ni.com/en-lb/support/model.ni-9213.html. [Accessed: 29- Feb - 2019].

[72] National Instrument, "C Series Current Input Module NI-9227," Available: http://www.ni.com/en-lb/support/model.ni-9227.html. [Accessed: 28 Feb 2019].

[73] National Instruments, "C Series Voltage Input Module NI-9221," Available: http://www.ni.com/en-lb/support/model.ni-9221.html. [Accessed: 28 Feb 2019].

[74] C. Elliott, V. Vijayakumar, W. Zink and R. Hansen, "National Instruments LabVIEW: A Programming Environment for Laboratory Automation and Measurement", Journal of the Association for Laboratory Automation, vol. 12, no. 1, pp. 17-24, 2007. Available: 10.1016/j.jala.2006.07.012.

[75] Davis Instruments, "Davis Instruments 6152 Vantage Pro 2 Wireless Weather Station," Available: http://www.davis.com/Product/Davis_Instruments_6152_Vantage_Pro_2_Wireless_Weather_Station/DO-86403-03. [Accessed: 01 March 2019].

[76] Apogee Instrument, "SP-110-SS: Self-Powered Pyranometer," Available: https://www.apogeeinstruments.com/sp-110-ss-self-powered-pyranometer/. [Accessed: 01 March 2019].

[77] Reotemp Instruments, "Thermocouple Info," Available: https://www.thermocoupleinfo.com/. [Accessed: 01 March 2019].

[78] RS components, "Thermocouple Wire Type K, -75 → +250 °C 1 Core Unscreened PTFE Sheath 25m," Available: https://uk.rs-online.com/web/p/products/3630389/. [Accessed: 03 March 2019].

[79] J. Allen, "Calibration of equipment and calibration curves," Europe PMC, vol. 17, no. 1, pp. 50-53, 2013. PMID: 23627247

[80] B. Rose, "How to Select a Peltier Module," 2018. Available: https://www.cui.com/blog/how-to-select-a-peltier-module.

[81] Banggood, "TEC1-12708 Heat Sink Thermoelectric Cooler Peltier Plate Module," Available: https://www.banggood.com/TEC1-12708-Heatsink-Thermoelectric-Cooler-Peltier-Plate-Module-p-1020994.html?cur_warehouse=CN. [Accessed: 03 March 2019].

[82] Global sources, "Heat Pipe Aluminum Heat sinks, Made of Anodized Aluminum, Heat sink for Industrial Equipment," Available: https://www.globalsources.com/gsol/I/Heatsink/p/sm/1085440491.htm#1085440491. [Accessed: 03 March 2019].

[83] Dynatron, "DC fan," Dynatron, Available: https://www.dynatron.co/product-page/92-x-92-x-25-mm-dc-fan. [Accessed: 04 March 2019].

[84] Ultracool, "UltraCool Evaporative Cellulose Cooling Pad for Symphony Hicool Air Cooler (Brown)," Available: https://www.amazon.in/UltraCool-Evaporative-Cellulose-Cooling-Symphony/dp/B074QNM3P8. [Accessed: 04 March 2019].

[85] Halnziye, "HY710 silver thermal grease syringe," Available: http://www.halnziye.net/products_detail/&productId=65.html. [Accessed: 04 March 2019].

[86] Banggood, "Mini Switching Power Supply 220V to 12V 20A 250W For LED Strip Light," Available: https://www.banggood.com/Mini-Switching-Power-Supply-220V-To-12V-20A-250W-For-LED-Strip-Light-p-1017261.html?rmmds=myorder&cur_warehouse=CN. [Accessed: 05 March 2019].

[87] SolarPower"PV Cleaning: Choosing the Optimal Method and Frequency", SolarPower Europe, 2017. Available: http://www.solarpowereurope.org/pv-cleaning-choosing-the-optimal-method-and-frequency/. [Accessed: 05 March 2019].

[88] TzahiV, "Cleaning of solar panel," 2015. Available: https://www.istockphoto.com/ae/photo/cleaning-of-solar-panels-gm488580550-74258373.

[89] Solar choice, "Solar panel cleaning: Why, how & how often?", 2016. Available: https://www.solarchoice.net.au/blog/solar-panel-cleaning-why-how-how-often. [Accessed: 05 March 2019].

[90] Renewable energy world, "Listen up: how often should I clean my solar panels?", 2014. Available:https://www.renewableenergyworld.com/articles/2014/05/listen-up-how-often-should-i-clean-my-solar-panels.html. [Accessed: 05 March 2019].

[91] A. Jones and C. Underwood, "A thermal model for photovoltaic systems", Solar Energy, vol. 70, no. 4, pp. 349-359, 2001. Available: 10.1016/s0038-092x(00)00149-3.

[92] S. Sharples and P. Charlesworth, "Full-scale measurements of wind-induced convective heat transfer from a roof-mounted flat plate solar collector", Solar Energy, vol. 62, no. 2, pp. 69-77, 1998. Available: 10.1016/s0038-092x(97)00119-9.

[93] A. Karafil, H. Ozbay, M. Kesler, "Temperature and solar radiation effects on photovoltaic panel power," Journal of new results in science, vol. 12, pp. 48-58, 2016. ISSN: 1304-7981

[94] A. Bouchalkha, "Modeling of Dust Effect on Solar Panels in Abu Dhabi," in The Second International Energy 2030 Conference, Abu Dhabi, 2008.

[95] A. Wilkinson, Compendium of chemical terminology, 2nd ed. Oxford: Blackwell, 2006.

[96] H. Harcourt, "Earth's Atmosphere," in Science book, Houghton Mifflin Harcourt Publishing Company, p. 660.

[97] UCAR, "Humidity," Available: https://scied.ucar.edu/shortcontent/humidity. [Accessed: 26 March 2019].

[98] A. Magrini, L. Cattani, M. Cartesegna and L. Magnani, "Water Production from Air Conditioning Systems: Some Evaluations about a Sustainable Use of Resources", Sustainability, vol. 9, no. 8, p. 1309, 2017. Available: 10.3390/su9081309.

[99] B. Robertson, "Why does air expand when you heat it, and why does hot air rise?", 17 08 2006. Available: https://www.nsta.org/publications/news/story.aspx?id=52428. [Accessed: 28 March 2019].

[100] X. Sun, Y. Sun, Z. Zhou, M. Alam and P. Bermel, "Radiative sky cooling: fundamental physics, materials, structures, and applications", Nanophotonics, vol. 6, no. 5, pp. 997-1015, 2017. Available: 10.1515/nanoph-2017-0020.

[101] M. Zeyghami, D. Goswami and E. Stefanakos, "A review of clear sky radiative cooling developments and applications in renewable power systems and

passive building cooling", Solar Energy Materials and Solar Cells, vol. 178, pp. 115-128, 2018. Available: 10.1016/j.solmat.2018.01.015.

[102] E. Natsheh and A. Albarbar, "Solar power plant performance evaluation: simulation and experimental validation", Journal of Physics: Conference Series, vol. 364, p. 012122, 2012. Available: 10.1088/1742-6596/364/1/012122.

[103] J. Ramos, J. Campayo, J. Larranga, E. Zulueta, O. Barambones, J. Motrico, U. Gamiz, I. Zamora, "Two photovoltaic cell simulation models in Matlab/Simulink," International Journal on “Technical and Physical Problems of Engineering”, vol. 4, no. 10, pp. 45-51, 2012, ISSN 2077-3528.

[104] F. Gonzalez-Longatt, "Model of Photovoltaic Module in Matlab," Personnel.univ-reunion.fr, pp. 1-5, 2006.

[105] T. Gibson and N. Kelly, "Solar photovoltaic charging of lithium-ion batteries", Journal of Power Sources, vol. 195, no. 12, pp. 3928-3932, 2010. Available: 10.1016/j.jpowsour.2009.12.082.

[106] A. Salman, M. Ibrahim, W. Mukhtar, M. Farooq, S. Ahmad S and M. Saad, "Comprehensive Overview of Basic Photovoltaic (PV) Power System," International Journal of Scientific & Engineering Research, vol. 5, no. 4, p. 7, 2014, ISSN 2229-5518.

[107] S. Ozdemir, N. Altin and I. Sefa, "Fuzzy logic based MPPT controller for high conversion ratio quadratic boost converter", International Journal of Hydrogen Energy, vol. 42, no. 28, pp. 17748-17759, 2017. Available: 10.1016/j.ijhydene.2017.02.191.

[108] W. Li and X. He, "Review of Nonisolated High-Step-Up DC/DC Converters in Photovoltaic Grid-Connected Applications", IEEE Transactions on Industrial Electronics, vol. 58, no. 4, pp. 1239-1250, 2011. Available: 10.1109/tie.2010.2049715.

[109] N. Hanisah, T. Nizar, F. Abdul Hamid, R. Ali and M. Irwanto, "Topologies of DC-DC Converter in Solar PV Applications", Indonesian Journal of Electrical Engineering and Computer Science, vol. 8, no. 2, p. 368, 2017. Available: 10.11591/ijeecs.v8.i2.pp368-374.

[110] Alternative energy sources, "Solar Cell I-V Characteristic," Available: http://www.alternative-energy-tutorials.com/energy-articles/solar-cell-i-v-characteristic.html. [Accessed: 11 April 2019].

[111] E. Durán, J. Andújar, J. Enrique and J. Pérez-Oria, "Determination of PV Generator I-V/P-V Characteristic Curves Using a DC-DC Converter

Controlled by a Virtual Instrument", International Journal of Photoenergy, vol. 2012, pp. 1-13, 2012. Available: 10.1155/2012/843185.